https://doi.org/10.5194/egusphere-2026-4630
Preprint. Discussion started: 6 August 2026

From Sensors to Irrigation Decisions: An Automated Data–Model Pipeline for Real-Time Soil Moisture Forecasting in Agriculture

Haojin Zhao[1,2], Richard Hoffmann[1,2], Heye Bogena[1], Cosimo Brogi[1], Alexandre Belleflamme[1,2], Klaus Görgen[1,2], Johannes Keller[1,2], Lukas Strebel[1,2], and Harrie-Jan Hendricks Franssen[1,2]

[1]Institute of Bio- and Geosciences: Agrosphere (IBG-3), Forschungszentrum Jülich, Jülich, 52425, Germany
[2]Centre for High-Performance Scientific Computing in Terrestrial Systems, HPSC TerrSys, Forschungszentrum Jülich, Jülich, 52425, Germany

Correspondence: Haojin Zhao (h.zhao@fz-juelich.de)

Abstract. Increasing water scarcity and climate variability demand reliable, site-specific soil moisture information to guide irrigation and crop management decisions at the plot scale. Land surface models simulate the interactions between land, vegetation, and the atmosphere, and provide detailed information on hydrological states and fluxes. This study presents an automated, end-to-end modelling pipeline that connects real-time sensor observation, land surface modelling, data assimilation, and ensemble forecasts to deliver operational, site-specific soil moisture forecasts for agricultural stakeholders. The framework integrates in situ measurements from a Cosmic-Ray Neutron Sensor (CRNS) with the Community Land Model version 5 (CLM5) and the Parallel Data Assimilation Framework (PDAF). Observations are assimilated using an Ensemble Kalman Filter (EnKF) to constrain model states and reduce uncertainties. For forecasting, the system includes medium-range ensemble weather predictions from the European Centre for Medium-Range Weather Forecasts (ECMWF), which provide probabilistic information on future atmospheric conditions by running multiple simulations with perturbed initial states. Applied at the Selhausen agricultural research site (Germany), the framework shows how data assimilation improves the agreement between simulated and observed soil moisture by approximately 20 % (e.g., reduced RMSE), and yields short-term forecasts with skill comparable to or exceeding the open-loop at short-to-intermediate lead times, with added value becoming particularly apparent when unresolved wetting or drying events occur later in the forecast horizon. By translating model outputs into threshold-based indicators, the system enables actionable insights for irrigation and field management, thereby bridging the gap between scientific modelling and practical agricultural decision-making. Overall, the proposed framework represents an important step towards an operational, site-specific decision-support tool for short-term irrigation and agricultural water management under uncertain weather conditions.

1 Introduction

Rising climate variability and the consequent rise in frequency and intensity of droughts significantly increase uncertainties in the management of agricultural water resources (Aaheim et al., 2012; Lobell and Gourdji, 2012; Reichstein et al., 2013; Pulido-Bosch et al., 2018; Raza et al., 2019; Klages et al., 2020; Fu et al., 2022). Global soil water systems are under unprecedented stress from population growth, agricultural intensification, and climate warming (Liu et al., 2022). There is thus a need for

https://doi.org/10.5194/egusphere-2026-4630
Preprint. Discussion started: 6 August 2026

effective and sustainable agricultural management practices supported by predictive tools that integrate real-time data and soil–water process models. Such tools could enable accurate, site-specific short-term irrigation and crop management decisions.

Low-cost wireless sensor networks and Internet-of-Things (IoT) devices enable remote monitoring and assessment of field-scale water and energy fluxes (Ochsner et al., 2013; Bogena et al., 2018; Freebairn et al., 2018; Brinkhoff et al., 2019; Li et al., 2020; Bwambale et al., 2022; Veerachamy and Ramar, 2022; Nsoh et al., 2024). At the same time, traditional land surface and hydrological models simulate water, energy, and carbon exchanges at different scales based on conservation laws and physically based parameterizations, which allows us to better understand the impact of climate variability on crop production (Karandish and Šimůnek, 2016; Lawrence et al., 2019; Colossi and Tucci, 2020; Boas et al., 2021; Li et al., 2024). However, uncertainty in meteorological forcing, model structure, initial states, and parameters often limits the predictive skills of these tools, and thus their usability.

Advances in data assimilation (DA) can improve model predictive capabilities by combining simulations with observational data, leading to improved predictions of states and fluxes that can better support agricultural practices, such as irrigation scheduling (Li et al., 2018; Colossi and Tucci, 2020; Gumiere et al., 2020; Togneri et al., 2022; Jin et al., 2022). One class of data assimilation approaches is based on sequential frameworks, in which model states are recursively updated as new observations become available. In this context, data assimilation provides a mathematically rigorous approach to combine prior model forecasts with observational data, thereby continuously correcting model trajectories over time (Reichle, 2008). This capability makes data assimilation suitable for operational land surface modelling under changing climatic conditions. By continuously integrating land information from observations (e.g., satellite retrievals and in situ measurements), data assimilation enables the dynamic updating of model states and improves the reliability of short-to-mid-term forecasts (Colossi and Tucci, 2020; Strebel et al., 2022; Li et al., 2024).

Beyond modelling and assimilation, there is a growing need to develop climate-resilient agricultural strategies that are supported by effective climate service frameworks and can translate scientific information into actionable knowledge for end-users. Climate services aim to provide tailored, decision-relevant information, such as soil moisture dynamics and drought risk, to support adaptation and resource management in agriculture (Raza et al., 2019; Srivastav et al., 2021; Alwis et al., 2022). However, the transition from a supply-driven provision of climate information to a demand-driven service remains challenging. A major challenge lies in the connection between scientific developments and stakeholder needs (Bojovic et al., 2021). In fact, the practical value of model outputs for agricultural decision-making depends not only on their scientific quality but also on how results are presented, interpreted, integrated into management practices, and weighed against their costs and benefits. Studies have shown that climate information is often produced at regional and global scales, while decisions are made at smaller local scales (Smith et al., 2021; Sadri et al., 2022). Additionally, such information is often presented in a manner that is tailored to expert users, while a broader audience struggles to interpret what is usable and relevant for their specific needs (Porter and Dessai, 2017). These mismatches contribute to a gap, limiting the effective use of climate information in practical applications. Consequently, there is an increasing demand for integrated, user-oriented systems that bridge this gap by combining high-quality modelling with application-focused outputs. To achieve this, model outputs must be translated into context-specific management information, such as irrigation recommendations or risk indicators, that can be easily interpreted by farmers

https://doi.org/10.5194/egusphere-2026-4630
Preprint. Discussion started: 6 August 2026

and agricultural stakeholders. In this context, automated data-model pipelines represent a promising but still underdeveloped approach for operational, plot-scale applications (Zhao et al., 2026a; Hendrickx et al., 2026). Therefore, this study presents an automated, end-to-end data-model pipeline for operational, site-specific soil moisture ensemble forecasting, designed to support agricultural stakeholders.

The pipeline presented in this study integrates in situ observations, cloud-based data processing, numerical modelling, and data assimilation to generate probabilistic site-specific forecasts based on ensemble weather forecasts. It consists of four main components: (i) an integrated observation system; (ii) automated data transmission, processing, and storage in the cloud infrastructure; (iii) numerical simulation and data assimilation using a land surface model, and (iv) user-oriented delivery of forecast information. At its core, the modelling framework builds upon the Community Land Model version 5 (CLM5) (Lawrence et al., 2019) coupled with the Parallel Data Assimilation Framework (PDAF) (Nerger et al., 2005), hereafter referred to as CLM5-PDAF (Strebel et al., 2022). The main contributions of this study are as follows:

- Automated data assimilation and forecasting: We extend the CLM5-PDAF system to continuously integrate cosmic-ray neutron sensors (CRNS) soil moisture estimates and local meteorological measurements. The system uses the Ensemble Kalman Filter (EnKF) to update soil moisture states, providing improved initial conditions for a 10-day forecast. By keeping all ensemble members in memory, the pipeline avoids costly re-initialisation and better supports real-time operation.

- Integration of ensemble weather forecasts: Atmospheric forcing for the forecast stage is derived from an ensemble of medium-range weather predictions generated by the European Centre for Medium-Range Weather Forecasts (ECMWF). Then, ensemble forecasts are generated over a 10-day horizon that propagate atmospheric uncertainty and enable probabilistic information on agricultural variables, such as soil moisture, soil temperature, and evapotranspiration.

- Translation to management recommendations: In addition to producing scientific model outputs, this pipeline provides a user-centred interface that translates forecast information into actionable guidance. Model outputs such as soil moisture at different depths are used in combination with predefined thresholds to derive management information (e.g., irrigation timing and quantity).

2 Materials and methods

2.1 Integrated observation system

At the monitoring site (see detailed description below), an integrated framework combines field-scale, point-scale, and meteorological observations to provide complementary information on soil and atmospheric conditions required for land surface modelling and data assimilation. It consists of three main components: (i) a cosmic-ray neutron sensor (CRNS), which provides spatially integrated estimates of soil moisture at the field scale; (ii) a distributed soil sensor network (SoilNet) that measures soil mositure and soil temperature at multiple depth for local validation and characterization of vertical soil water dynamics;

https://doi.org/10.5194/egusphere-2026-4630
Preprint. Discussion started: 6 August 2026

and (iii) an automated meteorological station that continuously records key atmospheric variables, such as precipitation, air temperature, humidity, wind, and radiation.

The CRNS monitors the surrounding environmental neutron intensity, which is inversely related to environmental hydrogen content (e.g., soil water) (Zreda et al., 2008; Andreasen et al., 2017). Compared with conventional point measurements, CRNS provides non-invasive and continuous field-scale estimates of volumetric soil moisture. The effective measured volume, or footprint, of a CRNS varies with air pressure, air humidity, soil moisture, and vegetation conditions. Typically, the footprint ranges between 150 m (wet) to 240 m (dry) in radius, with an effective sensing depth of several tens of centimeters (Köhli et al., 2015; Schrön et al., 2017). Nonetheless, half of the neutron signal is generally representative of the first 50 m around the sensor (Köhli et al., 2015). The potential of CRNS in irrigation management has been widely recognised (Franz et al., 2020; Ragab et al., 2017; Köhli, 2026; Brogi et al., 2022). However, its adoption in irrigation modelling frameworks remains limited, mainly due to methodological complexity and inconsistent performance in certain irrigated setups (Brogi et al., 2023, 2026).

To complement the field-scale CRNS observations, the SoilNet wireless sensor network provides high-resolution, point-scale measurements of soil moisture and temperature. In addition to these core sensing components, the monitoring system integrates front-end electronics and data acquisition units that process neutron detector signals and integrate observations from CRNS, SoilNet probes, and meteorological stations into a common data logger for synchronized recording and subsequent transmission (Ney et al., 2021).

2.2 Data transmission and cloud infrastructure

Measured data is transmitted via low-power wide-area communication technologies such as Narrowband Internet of Things (NB-IoT) and cellular networks, including mobile communication technologies (Bogena et al., 2022b). These technologies enable energy-efficient, robust, and near-real-time data transfer from agricultural monitoring sites to remote cloud infrastructure. The monitoring network combines measurements from multiple sensor systems operating at different temporal resolutions, and measurements are aggregated if needed and transmitted hourly by the station data logger (Ney et al., 2021). The logger synchronizes observations from the different sensor systems and performs initial processing steps, including filtering, formatting, and time synchronization. Upon arrival at the cloud server, automated processing workflows conduct quality control procedures, apply sensor-specific corrections, and derive higher-level products. For the CRNS, this includes correction of neutron count rates and conversion to soil moisture estimates following the harmonized processing framework of Bogena et al. (2022a). For meteorological variables, a standardized gap-filling procedure is applied within the data processing pipeline. Following quality control checks, short data gaps are filled using temporal interpolation, whereas longer gaps are reconstructed using observations from neighbouring stations. For each variable, a reduced major axis linear regression is fitted to overlapping quality-controlled observations, and the fitted regression coefficients are subsequently applied to neighbouring-station observations during periods when measurements at the target station are unavailable. Those gap-filled data are flagged in the database to ensure traceability. The processed data are then stored in structured databases and made available through a web-based platform - the TERENO Data Discovery Portal (https://ddp.tereno.net/ddp/) that supports near real-time visualization, analysis, and integration into numerical models for forecasting applications.

https://doi.org/10.5194/egusphere-2026-4630
Preprint. Discussion started: 6 August 2026

2.3 Numerical simulation and data assimilation

2.3.1 CLM5-PDAF

The latest version of the land component in the Community Earth System Model (CESM), CLM5, is used (Kay et al., 2015; Lawrence et al., 2019). CLM5 simulates water, energy, carbon, and nitrogen cycles within the terrestrial system. Soil hydrological processes are represented through a physically based formulation, where water movement in the vadose zone is described by a finite-difference approximation of the Richards equation combined with Brooks-Corey parameterization (Lawrence et al., 2019). Soil hydraulic properties are derived from pedotransfer functions (Clapp and Hornberger, 1978) based on the soil texture (e.g., sand and clay fractions) and organic matter content. CLM5 simulations are driven by atmospheric forcing data, including precipitation, relative humidity, air pressure, air temperature, wind speed, and radiation. The model can be applied at regional to global scales (Ma et al., 2023; Yan et al., 2023) or be configured in a single grid-cell mode. Studies have demonstrated the capability of CLM5 to incorporate self-collected hydrological and meteorological data (Wieder et al., 2017; Strebel et al., 2022), as well as complex agricultural management practices (Boas et al., 2021; Dombrowski et al., 2022). The CLM5-PDAF system is built within the Terrestrial Modelling Platform model (TSMP)(Shrestha et al., 2014), which provides a high-performance modelling environment for coupled atmosphere-land surface-subsurface simulations together with data assimilation workflows (TSMP-PDAF)(Kurtz et al., 2016). Within this architecture, PDAF acts as an external but tightly integrated software for data assimilation algorithms. The coupling follows an online strategy in which PDAF and CLM5 are compiled into a single executable using modified pseudo-library versions of the model. This design keeps model states in the main memory during runtime, avoiding costly file-based communication and repeated model re-initialization steps (Strebel et al., 2022). During runtime, CLM5 operates in ensemble mode, and PDAF routines are triggered through subroutines and stop-alarm mechanisms that define the model state vector and initiate the data assimilation step whenever new observations become available. Each ensemble member represents an independent realization with perturbed atmospheric forcing, model parameters, and initial conditions. Together, the spread across the ensemble quantifies the model uncertainty. The simulations in this study were performed on the high-performance computing (HPC) infrastructure of the Jülich Supercomputing Centre, but the framework is also portable to other Linux-based HPC environments.

2.3.2 Meteorological forcing from ECMWF forecast systems

Modern Land Surface Model (LSM) applications are driven by a variety of atmospheric forcing datasets. In this study, we use ECMWF products generated by its Integrated Forecasting System (IFS) as they provide multiple physically consistent realizations of real-time atmospheric forecasts. IFS produces a single high-resolution deterministic forecast (HRES), which is based on ECMWF's highest-resolution model and serves as a deterministic reference. However, it does not represent the uncertainty in atmospheric evolution, which arises from errors in initial conditions and model formulations. The Ensemble Prediction System (ENS) addresses this limitation through 50 perturbed forecast members, with hourly forecasts during the early forecast range (up to 90 hours), after which the temporal resolution is progressively reduced to 3 hourly for a forecast window between 93 and 114 hours and 6 hourly for a forecast window between 150 and 260 hours. The atmospheric forcing fields are provided at a $0.1^\circ \times 0.1^\circ$ resolution. When used as forcing for LSMs, each ensemble member generates an independent realization of land surface states, allowing probabilistic assessment of land surface states. The ensemble forecasts have been shown to provide informative forecasting and early warning systems (Ollinaho et al., 2021; Belleflamme et al., 2023; Casado-Rodríguez et al., 2025).

2.3.3 Data assimilation

Forecast uncertainties arise from imperfect initial conditions, (atmospheric) forcing data, and model structural errors (Turner et al., 2008). Data assimilation provides a statistical framework to quantify and reduce uncertainty related to initial and boundary conditions as well as model parameterization. In this pipeline, the Ensemble Kalman Filter (EnKF), implemented within CLM5-PDAF, is used to assimilate soil moisture observations derived from CRNS into the land surface model CLM5, thereby providing updated initial conditions for the forecast simulations. The EnKF is a sequential data assimilation method in which nonlinear dynamical systems are approximated stochastically using Monte Carlo ensembles. During the forecast step, the soil moisture state vector for ensemble member i at time step t is propagated forward in time following:

$$\mathbf{x}_{i,t} = \mathbf{M}\left(\mathbf{x}_{i,t-1}, \mathbf{u}, \mathbf{p}\right) \tag{1}$$

where $\mathbf{M}$ represents the nonlinear model operator, $\mathbf{x}_{i,t-1}$ is the analysis state from previous step, $\mathbf{u}$ represents uncertain atmospheric forcing inputs and $\mathbf{p}$ denotes perturbations associated with model parameters. When new observations become available, the forecast model states are updated through the EnKF analysis step:

$$\mathbf{x}^a_{i,t} = \mathbf{x}^f_{i,t} + \mathbf{K}_t\left(\mathbf{y}_{i,t} - \mathbf{H}_t\mathbf{x}^f_{i,t}\right) \tag{2}$$

where the superscripts a and f denote the analysis (updated) and forecast states, respectively, $\mathbf{y}_{i,t}$ is the observation vector, $\mathbf{H}_t$ is the linear observation operator mapping model states into observation space, and $\mathbf{K}_t$ is the Kalman gain matrix, which is computed as:

$$\mathbf{K}_t = \mathbf{P}_t\mathbf{H}_t^{\mathrm{T}}\left(\mathbf{H}_t\mathbf{P}_t\mathbf{H}_t^{\mathrm{T}} + \mathbf{R}_t\right)^{-1} \tag{3}$$

where $(\cdot)^{\mathrm{T}}$ denotes the transpose operator, $\mathbf{R}_t$ is the measurement error covariance matrix, and $\mathbf{P}_t$ represents the model forecast error covariance matrix that is approximated from the ensemble spread:

$$\mathbf{P}_t = \frac{1}{N-1}\sum_{i=1}^{N}\left(\mathbf{x}^f_{i,t} - \bar{\mathbf{x}}^f\right)\left(\mathbf{x}^f_{i,t} - \bar{\mathbf{x}}^f\right)^{\mathrm{T}} \tag{4}$$

where N denotes the total number of ensemble members. Further details on the numerical implementation and calculation routines within CLM5-PDAF are provided by Strebel et al. (2022).

https://doi.org/10.5194/egusphere-2026-4630
Preprint. Discussion started: 6 August 2026

2.4 Stakeholder interaction and information delivery

The final stage of the data processing pipeline addresses the interaction between processed data products and end users. This layer is realized through web-based platforms and interactive dashboards, which provide near real-time access to observational data and model forecasts. Core functionalities of these platforms include: (i) real-time monitoring dashboards, displaying observed and modelled variables such as soil moisture, soil temperature, and evapotranspiration, providing continuous insight into current field conditions; (ii) forecast visualization tools, presenting ensemble-based predictions and uncertainties; and (iii) threshold-based alert and notification systems, which automatically inform users when critical conditions, such as drought stress or excessive soil moisture, are detected.

3 Case study: Selhausen

The agricultural research station Selhausen is located in western Germany within a managed cropland landscape of the Lower Rhine Valley (see Figure 1). It is situated at 104 m above sea level (a.s.l.), and the regional climate is classified as temperate maritime, characterized by moderate temperature and annual precipitation of approximately 700 mm (Pütz et al., 2016; Jarvis et al., 2022; Korres et al., 2015). The crop rotation comprises winter cereals (winter wheat and winter barley), cover crops, potatoes, and sugar beet (Brogi et al., 2025). The dominant soil type is Haplic Luvisol developed on aeolian deposits (Rudolph et al., 2015). According to Brogi et al. (2019), the central and eastern parts of the investigated field are composed of meters-deep aeolian sediments (generally, 14% sand, 67% silt, and 19% clay). The western side is characterized by similar aeolian sediments until around 1m depth, below which compacted sand and gravel are found. Overall, the area monitored by the CRNS is rather homogeneous in terms of soil characteristics (Brogi et al., 2025). The topsoil of the field exhibits an organic carbon content of 0.98 % and an average bulk density of 1.26 $\mathrm{g \cdot cm^3}$ (Wang et al., 2020; Boas et al., 2021).

Figure 2 provides an overview of the integrated monitoring, modelling, data assimilation, and forecasting system developed for the Selhausen site. Each ensemble member is configured through individualized namelist files using identifier suffixes to enable independent handling of forcing and input parameter perturbations. The model domain consists of a one-dimensional (1D) grid column with a spatial resolution of 100 m $\times$ 100 m, centered at the Selhausen CRNS station (Figure 1-d). The land surface is represented as 100 % cropland, with the crop functional type defined as rainfed potato, consistent with the actual land cover during the 2022 growing season. In the default CLM5 crop parameterization, potato does not have a dedicated parameter set and is represented using the winter wheat parameters. To better represent potato growth, we adopted the crop-specific potato parameterization developed by Boas et al. (2021), which includes revised phenological and physiological parameters (e.g., planting and harvest dates, maximum leaf area index, canopy height, and carbon allocation) based on field observations. Note that the year 2022 was characterised by anomalously low precipitation (568 mm compared to a long-term average of approximately 700 mm per year). Potato irrigation was applied during the growing season; however, irrigation timing and applied amounts were not recorded.

https://doi.org/10.5194/egusphere-2026-4630
Preprint. Discussion started: 6 August 2026

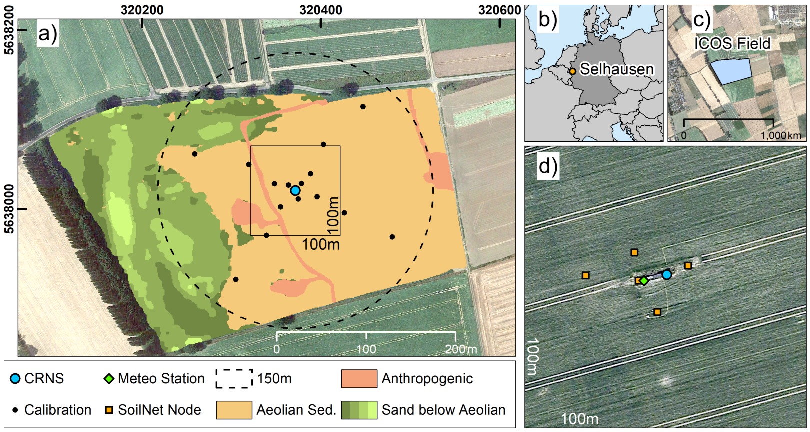

Figure 1. (a) Soil types around the agricultural research station Selhausen, with (b) its location in central Europe, (c) and extended view on its surrounding area, and (d) locations of the CRNS, meteorological station, and SoilNet nodes of the wireless sensor network. The background of panel a) shows a geophysics-based digital soil map of the site (Brogi et al., 2019). Satellite imagery: © Google, Maxar Technologies (2020, 2022).

3.1 Data

3.1.1 In situ measurements

The Selhausen site is part of the TERrestrial ENviromental Observatories (TERENO) network (Bogena et al., 2018) and has been operated as an Integrated Carbon Observation System (ICOS) Class 1 ecosystem station. It combines continuous measurements of soil moisture, soil temperature, meteorological conditions, and ecosystem fluxes. At this site, a CRNS (CRS-1000, Hydroinnova LLC, Albuquerque, NM, USA) has been operating continuously since 2015, recording raw neutron count rates at 10 min intervals. Currently, raw observations are automatically transferred to a cloud-based database. Here, by using the processing framework of Bogena et al. (2022a), raw counts are a) filtered, b) corrected for atmospheric pressure, air humidity, and incoming neutron influences (Desilets and Zreda, 2003; Rosolem et al., 2013; Hawdon et al., 2014), c) aggregated by using a 24-hour rolling mean, and d) converted into soil moisture estimates using the Desilets et al. (2010) method, expressed according to Köhli et al. (2021). A biomass correction (e.g., Baatz et al. (2015)) was not applied as no sufficient information on biomass development was available and because the influence of low-height annual crops is generally rather low (McJannet et al., 2014). The instrument calibration strategy followed Schrön et al. (2017), with sample locations shown in Figure 1-a. The resulting time series provide spatially integrated estimates of soil moisture over the CRNS footprint and are shown in Figure 3.

The accompanying SoilNet wireless sensor network has also operated since 2015 and consists of five monitoring nodes distributed within approximately 30 m of the CRNS station (Bogena et al., 2018). Each node is equipped with SMT100 sensors (Trübner GmbH, Neustadt, Germany) installed at depths of 5, 10, 20, 50, and 100 cm. All sensors were calibrated to convert raw output to dielectric permittivity (Bogena et al., 2017), which was subsequently related to soil water content using an empirical

https://doi.org/10.5194/egusphere-2026-4630
Preprint. Discussion started: 6 August 2026

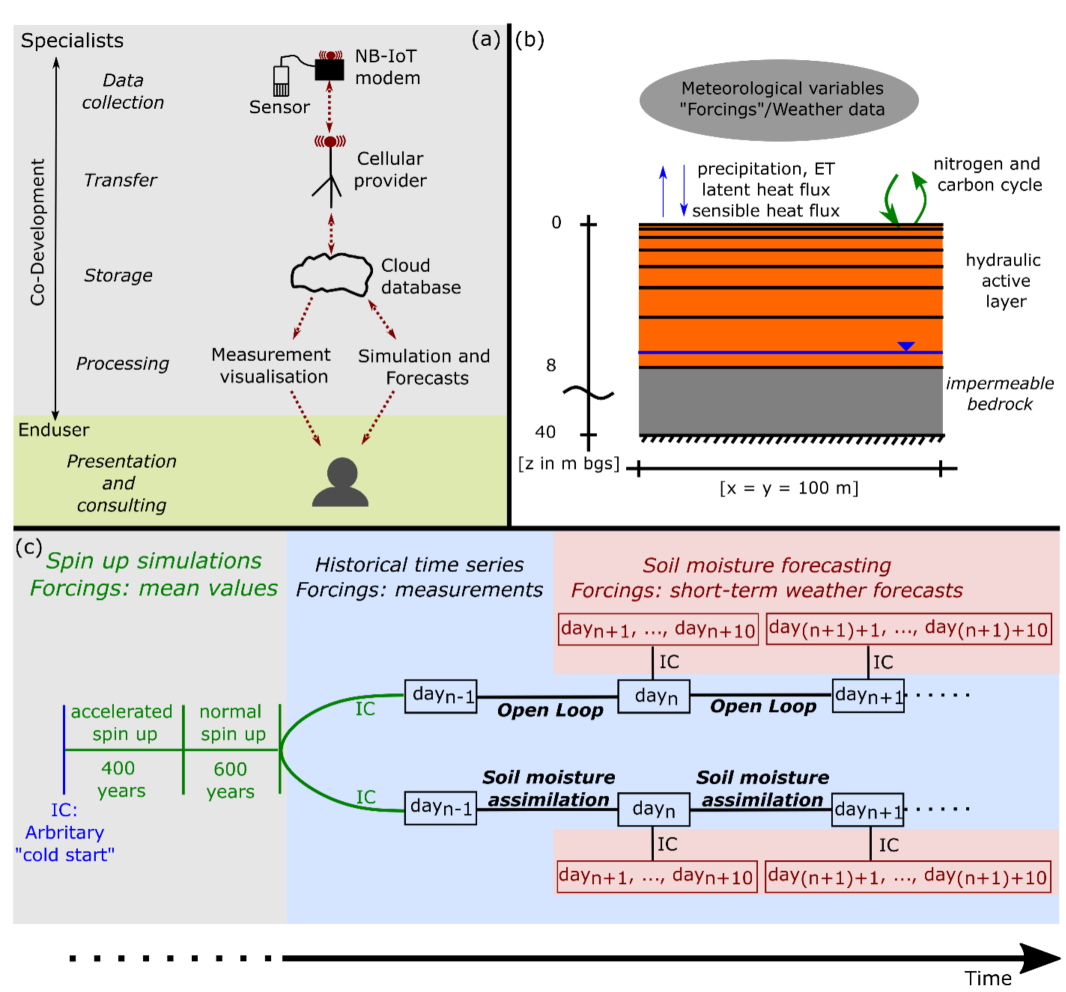

Figure 2. Schematic overview of the monitoring, modelling, and forecasting framework developed for site-specific soil moisture prediction at the Selhausen field site. a) Data acquisition and processing chain; b) Conceptual representation of the modelled soil column; c) Temporal workflow of the modelling system.

relationship (Topp et al., 1980). Because the site is actively managed for agricultural production, SoilNet sensors are generally removed before invasive field operations such as tillage or harvesting and subsequently reinstalled at the same locations.

In this case study, the CRNS soil moisture data were assimilated to constrain the model state vector, whereas point-scale soil sensor measurements were used for independent validation. Meteorological forcing data were obtained from the co-located ICOS station, including precipitation (OTT Pluvio^2 weighing rain gauge, Ott HydroMet, Kempten, Germany), air temperature and relative humidity (HC2S3, Rotronic, Bassersdorf, Germany), atmospheric pressure (PTB110 barometer, Vaisala Inc., Helsinki, Finland), incoming and outgoing shortwave radiation together with incoming and outgoing longwave radiation (CNR4 four-component net radiometer, Kipp & Zonen, Delft, The Netherlands), and wind observations.

https://doi.org/10.5194/egusphere-2026-4630
Preprint. Discussion started: 6 August 2026

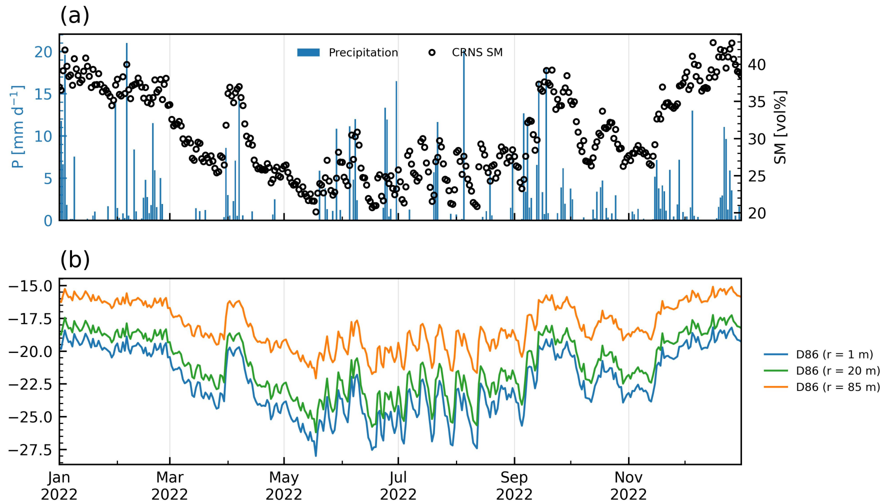

Figure 3. a) Daily time series of precipitation measured at the Selhausen site, and soil moisture derived from the cosmic-ray neutron sensor (CRNS) and b) estimated measurement depth for three radial distances from the sensor (i.e., 1, 20, and 85 m). The estimated measurement depths (D86) are calculated by using Schrön et al. (2017).

3.1.2 Atmospheric forcing

Atmospheric forcing data for the simulations were derived from two sources, depending on whether retrospective or predictive simulations were conducted. For simulations representing past conditions, in situ meteorological observations from the EC station at the Selhausen site were used. The continuous hourly observations cover the period from January 2011 to December 2022 and were quality-controlled and gap-filled following the processing procedures described by Graf et al. (2020) (see Figure 4). For predictive simulations, i.e., the generation of 10-day soil moisture forecasts, atmospheric forcing was instead provided by the ENS product from the ECMWF (see Figure 5). The spread of the ensemble increases with forecast lead time, reflecting the growing uncertainty due to the chaotic nature of the atmosphere and model limitations. Importantly, the ensemble can represent extreme or less likely conditions (e.g., heavy precipitation or drought events).

3.2 Perturbation

To account for uncertainties in model parameters, initial conditions, and meteorological forcing, an ensemble-based perturbation approach was applied. Such stochastic perturbations are commonly used in land surface data assimilation systems to represent model uncertainty and to generate a spread of plausible system states (Reichle, 2008; Gehne et al., 2019). Soil hydraulic properties, including sand, clay, and organic matter contents, were perturbed independently for each ensemble member by sampling from a uniform distribution with zero mean and a range of $\pm 20\%$ around their nominal values. To ensure physical consistency, cases where the sum of sand and clay fractions exceeded 100 $\%$ were re-scaled to unity following the

https://doi.org/10.5194/egusphere-2026-4630
Preprint. Discussion started: 6 August 2026

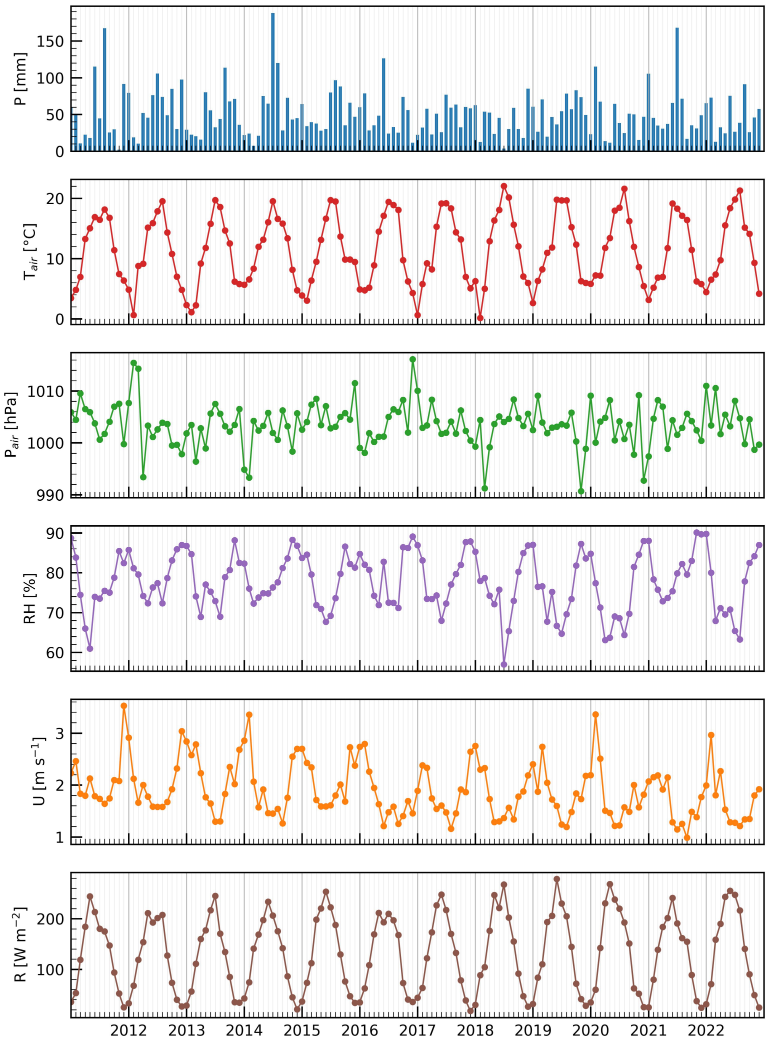

Figure 4. Meteorological observations aggregated at the monthly time scale observed at the Selhausen site. Shown are the monthly sum of precipitation (mm), average monthly 2 m temperature (T_{air}), average monthly 2 m air pressure (P_{air}), average monthly relative humidity (RH), average monthly 2 m wind speed (U), and average monthly global radiation (R).

approach of Strebel et al. (2022). Meteorological forcing uncertainty from the EC-station data was represented through perturbing precipitation, shortwave radiation, and air temperature using a multivariate stochastic framework that preserves prescribed cross-variable correlations (Reichle et al., 2007; Han et al., 2014). Precipitation and shortwave radiation were perturbed using a multiplicative log-normal distribution, and air temperature was perturbed using an additive Gaussian noise model, consistent with common practices in land data assimilation systems (Reichle et al., 2010; McMillan et al., 2011). The meteorological

https://doi.org/10.5194/egusphere-2026-4630
Preprint. Discussion started: 6 August 2026

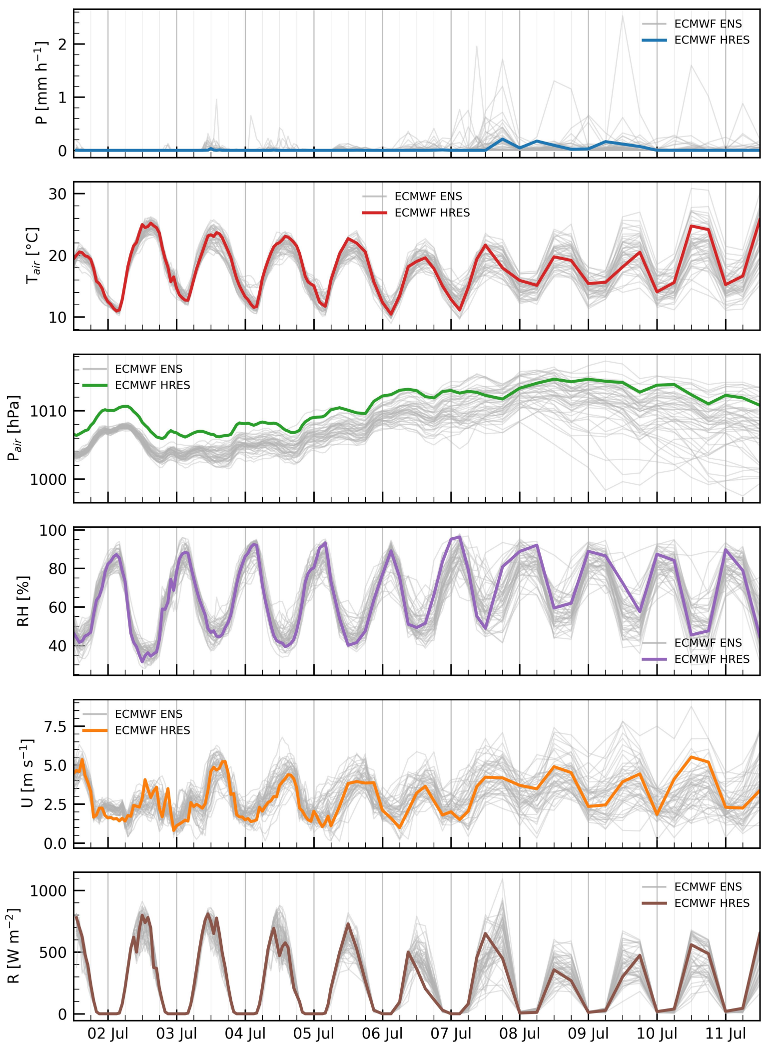

Figure 5. Example of an ensemble medium range weather forecast by ECMWF (initialized on 1 July 2022, 12:00 UTC) used as input for the Selhausen site. Precipitation (P), Air temperature (T_{air}), air pressure (P_{air}), relative humidity (RH), wind speed (U), and global radiation (R) are shown. Grey lines represent the 50 ensemble members (ENS), while the colored line denotes the high-resolution deterministic forecast (HRES).

measurements from the EC-station (see Figure 4) were aggregated to time steps of 1 hour before perturbation. The stochastic perturbation parameters used in this study are summarized in Table 1.

https://doi.org/10.5194/egusphere-2026-4630
Preprint. Discussion started: 6 August 2026

Table 1. Stochastic parameters used for perturbation of the meteorological in-situ measurements of precipitation, global radiation, and air temperature.

Perturbation	Multiplicative(M) or Additive(A)?	Mean	Std Dev	Correlations		
				P	R	T_{air}
Precipitation (P)	M	1.0	0.5	-	-0.8	0
Global radiation (R)	M	1.0	0.3	-0.8	-	0.4
Air temperature (T_{air}) (unit: K)	A	0.0	1.0	0	0.4	-

[a] Std Dev refers to standard deviation.

3.3 Spin-up

In this study, each data assimilation ensemble member was configured in eCLM biogeochemical (BGC) mode, in which the carbon and nitrogen cycles are explicitly represented, and the vegetation status, such as the leaf area index (LAI), evolves dynamically in response to environmental conditions. In models like CLM5, an extensive spin-up procedure is required to bring slow biogeochemical pools into equilibrium with the prescribed climate forcing (Lawrence et al., 2019). As these slow biogeochemical processes influence vegetation growth, transpiration, and root water uptake, an inadequate spin-up can also affect simulated soil moisture dynamics and hydrological fluxes. For this, a multi-stage spin-up strategy was applied. The model was initialized from arbitrary initial conditions and forced with repeated atmospheric data (1990 to 2010) from the CRUNCEPv7 (Viovy, 2018) dataset. The spin-up was conducted over 1000 simulation years. During the first phase, the model was run in accelerated deposition (AD) mode for 400 years, and a second spin-up phase of 600 years was performed under standard model settings. This strategy resulted in a near-equilibrium state of the terrestrial carbon and nitrogen pools with residual imbalances reduced to below approximately 5 % after about 900-1000 years of simulation.

3.4 Soil moisture assimilation

Simulations were performed with a model time step of 30 min, initialized from the equilibrated states of each ensemble member. This time step was retained to remain consistent with the standard CLM5 configuration. CLM5 can operate using forcing data with a coarser temporal resolution than its internal time step. We conducted both the data assimilation experiment and a reference simulation (open loop) for the year 2022. The EnKF is applied once per day at 12:00 UTC to assimilate soil moisture observations derived from CRNS, with a measurement uncertainty of 0.02 $cm^3 \cdot cm^{-3}$. This prescription is consistent with uncertainty estimates reported for CRNS-derived soil moisture observations and lies within the range typically obtained after temporal aggregation of neutron counts (Jakobi et al., 2020). The CRNS observation operator was implemented following Schrön et al. (2017) to ensure a consistent comparison between simulated and observed soil moisture. The effective measurement depth (D_{86}) was computed as a function of soil bulk density, soil moisture, and horizontal footprint radius (1, 20, and 85 m). Based on this depth, an exponential vertical weighting function was applied to discretized soil layers (1 mm resolution up to 0.92 m depth). These weights were then aggregated to the model's soil layers and normalized. The resulting

https://doi.org/10.5194/egusphere-2026-4630
Preprint. Discussion started: 6 August 2026

layer-specific weights were used to calculate a vertically weighted average soil moisture from the model state and also to distribute the observation increments across the soil column.

3.5 Forecast mode

290 Soil moisture forecasts are initialized from the model states obtained at the end of the data assimilation experiment (or from the open-loop simulation). The model is then integrated forward using a 30-minute internal time step and driven by the ECMWF ensemble weather forecasts described in Section 2.3.2. Forecasts are initialized once per day using the 12:00 UTC ECMWF ENS cycle, while the assimilation cycle is completed before the forecast initialization to provide the corresponding initial states.

3.6 Assessment of model performance

The performance of simulation experiments was evaluated using the root mean square error (RMSE), the mean bias error (MBE) and the Pearson correlation coefficient (r), defined as:

$$\mathrm{RMSE} = \sqrt{\frac{1}{N}\sum_{t=1}^{N}\left(\theta_{\mathrm{sim,t}} - \theta_{\mathrm{obs,t}}\right)^2} \tag{5}$$

$$\mathrm{MBE} = \frac{1}{N}\sum_{t=1}^{N}\left(\theta_{\mathrm{sim,t}} - \theta_{\mathrm{obs,t}}\right) \tag{6}$$

300 $$r = \frac{\sum_{t=1}^{N}\left(\theta_{\mathrm{sim,t}} - \overline{\theta}_{\mathrm{sim,t}}\right)\left(\theta_{\mathrm{obs,t}} - \overline{\theta}_{\mathrm{obs,t}}\right)}{\sqrt{\sum_{t=1}^{N}\left(\theta_{\mathrm{sim,t}} - \overline{\theta}_{\mathrm{sim,t}}\right)^2}\sqrt{\sum_{t=1}^{N}\left(\theta_{\mathrm{obs,t}} - \overline{\theta}_{\mathrm{obs,t}}\right)^2}} \tag{7}$$

where $\theta_{\mathrm{sim,t}}$ and $\theta_{\mathrm{obs,t}}$ denote the simulated and observed soil moisture at time step t, respectively, $\overline{\theta}_{\mathrm{sim,t}}$ and $\overline{\theta}_{\mathrm{obs,t}}$ are their temporal means, and N is the total number of time steps.

4 Results

4.1 Improvements for model simulations

305 Figure 6 presents a comparison between CRNS soil moisture observations and model simulations from the open-loop (OL) and data-assimilation (DA) experiments for the year 2022. The temporal dynamics (Figure 6 a) show that both simulations capture the seasonal patterns of soil moisture, characterized by wetter conditions during winter and early spring ($\approx$ 35-45 $vol\%$) and drier conditions during summer ($\approx$ 20-30 $vol\%$). However, the OL simulations generally overestimate soil moisture estimated by the CRNS, particularly during wet periods, while also showing underestimations during summer months. In comparison, the

https://doi.org/10.5194/egusphere-2026-4630
Preprint. Discussion started: 6 August 2026

DA simulation avoids these deviations and demonstrates a higher consistency with observed soil moisture dynamics than the OL. The scatter plots further quantify the agreement between simulations and observations (Figure 6 b-c). The OL simulation exhibits a relatively strong correlation with observations (Pearson r = 0.81) but with a noticeable wet bias (MBE = 1.43 $vol\%$) and higher overall error (RMSE = 4.85 $vol\%$). The DA simulations show improved performance, with a higher correlation (r = 0.90), reduced RMSE (2.76 $vol\%$), and a near-zero bias (MBE = -0.41 $vol\%$). The density of points is more closely distributed around the 1:1 line, indicating a more balanced representation and reduced seasonal biases across the full soil moisture range.

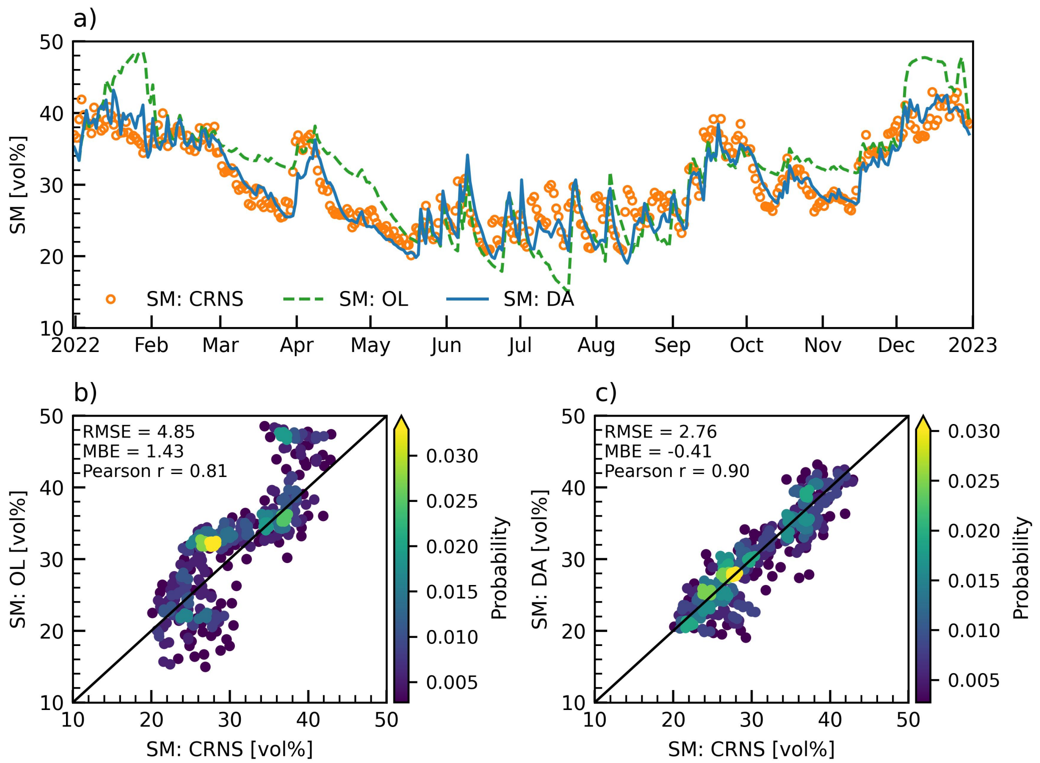

Figure 6. Comparison of CRNS-derived soil moisture (SM) observations with model simulations from the open loop (OL) and data assimilation (DA) experiments: a) Time series of SM, showing CRNS observations as orange circles, OL simulation (green dashed line), and DA simulation (blue dotted line); b)-c) Scatter plots of simulated versus observed SM for b) OL and c) DA. Colors indicate the probability density of point occurrence, and the 1:1 line is shown in black.

Figure 7 presents a comparison between simulated soil moisture and independent SoilNet point-scale observations at depths of 5, 10, 20, 50, and 100 cm. The simulated soil moisture reproduces the seasonal cycle across all depths, with drying during late spring-summer and wetting in autumn-winter, but exhibits systematic biases relative to point-scale observations. The OL simulation shows a pronounced wet bias in the upper and intermediate layers (5-20cm), with moderate to high correlations (Pearson r $\approx$ 0.86-0.92). DA improves performance by reducing both MBE and RMSE, but the improvements are more lim-

https://doi.org/10.5194/egusphere-2026-4630
Preprint. Discussion started: 6 August 2026

ited within the 5–20 cm layers. The impact of DA at depths of 50 cm and 100 cm occasionally degrades model performance as measured by RMSE, despite the relatively small bias at these depths. This depth-dependent improvement indicates that the assimilation of CRNS observations primarily improves near-surface soil moisture, consistent with the dominant sensing depth of approximately 10-20 cm at this site and the vertical weighting applied during the assimilation. The model appears to propagate assimilation increments more strongly into deeper layers than the measurements, suggesting that the model underestimates vertical hydraulic heterogeneity in the soil profile. The 100 cm layer is often near saturation, while observations at the EC station indicate that the water table depth generally oscillates between 2 and 2.5 m (Brogi et al., 2021). This suggests relatively shallow groundwater conditions, under which deeper soil moisture dynamics may be influenced by upward capillary supply from the groundwater table. CLM5 represents vertical soil water redistribution through matric-potential gradients; it does not prescribe the observed shallow water table as a lower boundary condition or simulate capillary rise from groundwater. Several deviations between simulations and SoilNet observations were observed during the study period. A sharp decline in measured soil moisture occurred in May 2022, coinciding with the temporary removal and subsequent re-installation of most sensors during field ploughing. Low soil moisture values were recorded after re-installation. In addition, CRNS measurements showed higher soil moisture values than point-scale sensors during parts of the summer period. The explanations for these discrepancies are discussed in the section 5.

Figure 8 shows the comparison between simulated and observed soil temperature at depths of 5, 10, 20, 50, and 100 cm. Both the OL and DA reproduce the seasonal cycle, capturing the warming from winter to summer and subsequent cooling towards winter across all depths. Model performance is consistently high, with strong correlations (Pearson r ≈ 0.93-0.96), moderate RMSE (≈ 2-4 °C) and small positive biases (MBE ≈ 0.6-1.5 °C) compared to previous studies (Lawrence et al., 2019; Ma et al., 2023). The agreement improves slightly with depth, reflecting increased thermal inertia and reduced short-term variability in deeper soil layers. Compared to OL, DA yields only marginal improvements in Pearson r, while slightly degrading performance in terms of MBE and RMSE. This limited response is likely because only soil moisture was directly assimilated, while soil temperature was adjusted only indirectly through model coupling. Although changes in soil moisture can influence soil heat capacity, thermal conductivity, evaporation, and surface energy partitioning, the strength of this coupling depends on the land-surface model's thermal and hydraulic parameterizations (in this case, CLM5). Consistent with this, other studies have similarly found that improvements in soil moisture estimates do not necessarily translate into corresponding improvements in soil temperature simulations (Alavi et al., 2009; Gevaert et al., 2018). The systematic seasonal bias, with overestimation of soil temperature in late summer–autumn and underestimation in winter, indicates a too large seasonal temperature amplitude in the model, which could be related to too high thermal conductivity or, for example, too low LAI in the model.

4.2 Forecast of decision-relevant variables

Figure 9 shows an example of a site-specific forecast initialized on 1 July 2022 at 12:00 UTC, spanning a short past window followed by a 10-day forecast horizon. Two distinct ensembles underlie the figure. The forecasts were initialized using model states derived from either the OL or the DA experiment and were driven by the operational weather forecast. For evaluation purposes, modelled soil moisture is compared with corresponding CRNS observations, although such observations would not

https://doi.org/10.5194/egusphere-2026-4630
Preprint. Discussion started: 6 August 2026

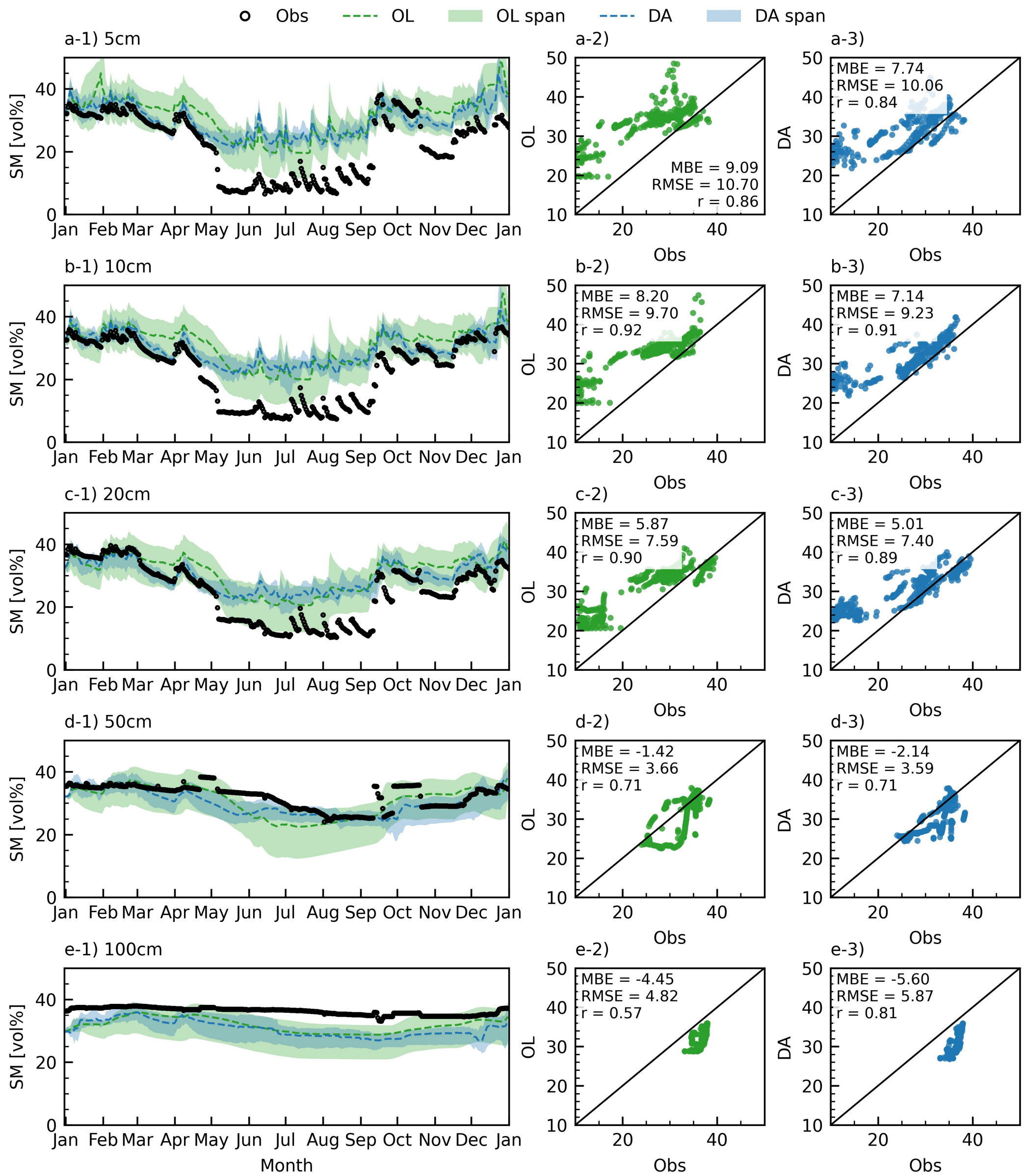

Figure 7. Comparison of observed soil moisture (SM) from in-soil sensors and simulated soil moisture from the open loop (OL) and data assimilation (DA) experiments at five depths (5, 10, 20, 50, and 100 cm). For each depth, the left panels (a-1 to e-1) show time series of observations (circles), open-loop simulations (OL, green), and data assimilation results (DA, blue), with shaded areas representing ensemble spread. The middle (a-2 to e-2) and right panels (a-3 to e-3) show scatter plots comparing observations with OL and DA, respectively.

https://doi.org/10.5194/egusphere-2026-4630
Preprint. Discussion started: 6 August 2026

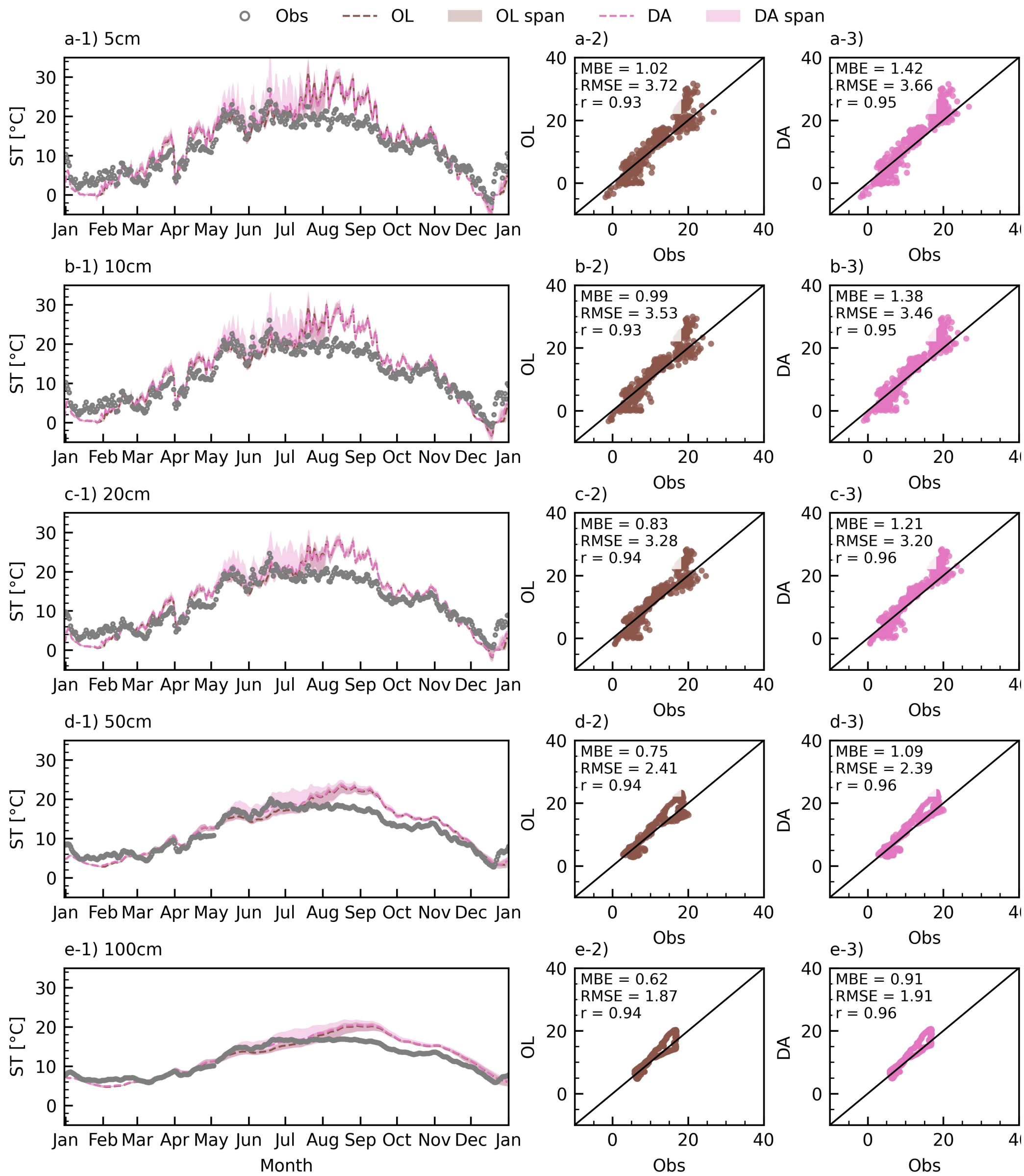

Figure 8. Comparison of observed soil temperature (ST) from in-soil sensors and simulated soil temperature from the open loop (OL) and data assimilation (DA) experiments at five depths (5, 10, 20, 50, and 100 cm). For each depth, the left panels (a-1 to e-1) show time series of observations (circles), open-loop simulations (OL, brown), and data assimilation results (DA, rosa), with shaded areas representing ensemble spread. The middle (a-2 to e-2) and right panels (a-3 to e-3) show scatter plots comparing observations with OL and DA, respectively.

https://doi.org/10.5194/egusphere-2026-4630
Preprint. Discussion started: 6 August 2026

be available in an operational forecasting setting. Panel (a) presents soil moisture in CRNS footprint space, as this corresponds to the observation type assimilated in the DA experiment and is therefore more representative for forecast verification than point-scale measurements. During the past period, the wetting response following the rainfall event on 30 June ($\sim$16 mm recorded at the on-site gauge) is evident in the CRNS signal. Both forecasts reproduce the overall drying–wetting sequence during this period, although their agreement with the CRNS observations varies with lead time. A further wetting episode around 6 July, present in the CRNS observations only, does not coincide with any gauge-recorded rainfall, as the period from 3–6 July was dry at the EC station. This observed wetting signal on the evening of 5 July in the absence of a corresponding rainfall event suggests a possible localized irrigation input. Since information on the timing and amount of irrigation is not available, as noted previously, this hypothesis cannot be independently verified. Note that as shown in Figure 6, the DA experiment is nonetheless able to partially correct for this unaccounted input, improving agreement with the observed soil moisture relative to the open-loop forecast.

The widening of the daily uncertainty range with forecast lead time reflects the increasing spread of the DA ensemble members. The spread originated from two sources: i) the perturbed soil properties, and ii) the divergence of the atmospheric forcing among the ENS members. The forecast initialized with DA has a moderate spread over the first few forecast days (spread $\sim$ 8.4 = 12.5 $vol\%$ for lead 0-4 days). From lead day 5 onward, the spread increases up to $\sim$ 17 $vol\%$ by day 9-10. This increase coincides with the period during which the ensemble precipitation forecasts diverge most strongly, although precipitation remains predominantly low to moderate and the probability of substantial rainfall is limited on most days. Atmospheric forcing is therefore considered the dominant, but not the only source of forecast uncertainty at longer lead times.

4.3 Towards climate service framework

While site-specific forecasts of soil moisture and related variables provide more information than conventional weather forecasts (e.g., precipitation and temperature), their direct interpretation remains challenging for non-expert users. Figure 9 presents physically consistent but scientifically oriented diagnostics, from which actionable insights may not be immediately apparent to stakeholders. A common approach in agricultural decision support systems is the use of threshold-based classification schemes to simplify complex soil moisture dynamics into management-relevant categories. We therefore translate forecasts of volumetric soil moisture into four regimes from a management perspective rather than soil hydraulic categories.

For silt-loam soils such as those at Selhausen, the FAO-56-based estimates for the surface layer are approximately 9–21 $vol\%$ for wilting point, 15.5–28.5 $vol\%$ for the critical soil moisture content, and 22–36 $vol\%$ for field capacity. As these ranges are rather large, we also considered the lysimeter-based study of Lu et al. (2026), who examined the critical soil moisture content separating energy-limited from water-limited evapotranspiration regimes across several German TERENO sites, including its variation with soil depth, texture, and climate. Lu et al. (2026) reported a surface critical soil moisture content of approximately 19-21 $vol\%$ and a root-zone critical soil water content of approximately 17 $vol\%$ for Selhausen, representing the point at which evapotranspiration becomes limited and drought stress begins. As the forecasts evaluated here represent soil moisture in the upper 10 cm, the surface-layer threshold is more appropriate than the root-zone value. We therefore use 22 $vol\%$ as the boundary between water-limited and favorable conditions. The lower threshold represents severe drought conditions and is

https://doi.org/10.5194/egusphere-2026-4630
Preprint. Discussion started: 6 August 2026

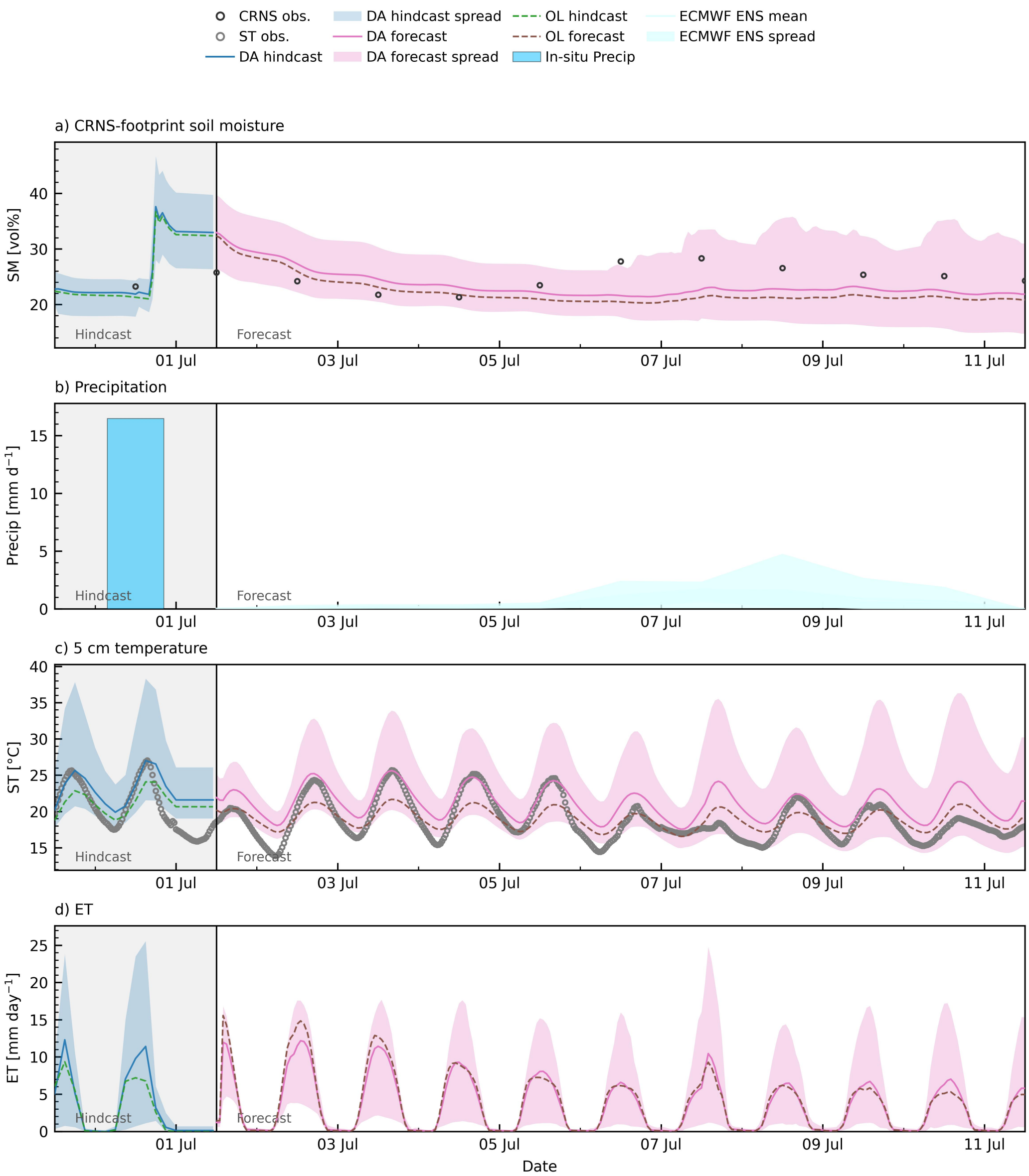

Figure 9. Forecast of land surface variables initialized on 1 July 2022 at 12:00 UTC, including a) soil moisture over the CRNS footprint, b) daily precipitation, c) soil temperature (ST) at 5 cm, and d) evapotranspiration (ET). Note that the DA experiment assimilated observations only before the forecast initialization time, and assimilation was discontinued at 12:00 UTC on 1 July 2022. Forecasts are shown for the OL- and DA-initialized experiments (Forecast$_{OL}$ OL and Forecast$_{DA}$ (DA), both driven by the ECMWF ENS atmospheric forcing, with ensemble means (lines) and ensemble spread (shaded areas).

https://doi.org/10.5194/egusphere-2026-4630
Preprint. Discussion started: 6 August 2026

associated with the permanent wilting point at approximately pF=4.2, which was calculated from the adopted van Genuchten soil-water retention curve and is approximately 10 $vol\%$. At the wet end, the main management limitation is the reduced traffic-ability of the field for heavy agricultural machinery. This threshold is associated with approximately pF=1.8, which corresponds to about 42 $vol\%$. For decision-support purposes, the hourly soil-moisture forecasts shown in Figure 9 are aggregated into daily mean values. These daily means are then classified into four regimes for the 10 cm surface layer, as shown in Figure 10: (i) below 10 $vol\%$ (too dry, high risk of plant damage); (ii) 10-22 $vol\%$ (drying, irrigation needed); (iii) 22-42 $vol\%$ (favourable); and (iv) $>$ 42 $vol\%$ (excessively wet, potentially restricted field traffic-ability). Daily-averaged surface soil moisture forecasts can thus be mapped directly onto these regimes to assess near-surface moisture conditions.

For the example forecast initialized on 1 July 2022, surface soil moisture was initially close to the lower boundary of the favourable range, with daily mean values of approximately 22 $vol\%$ on 29–30 June. Following the post-rainfall wetting, the ensemble mean rose on 1–2 July (approximately 25–26 $vol\%$), indicating favourable field conditions. Hereafter, soil moisture declined progressively to 24.1, 23.1, 22.5, and 22.1 $vol\%$ from 3 to 6 July, although critically dry conditions are not reached within the displayed forecast horizon. The ensemble-based category probabilities provide additional information beyond the daily mean. Across all forecast ensemble members, 84 % remained within the favourable category, while 16 % entered the drying category. The overall field condition is therefore classified as 'favourable', but with a trend towards drier conditions. Compared with the direct time-series representation shown in Figure 9, the threshold-based visualization highlights not only the expected soil moisture levels but also their management relevance. Such information can support operational decisions by indicating if and for how long soil moisture is expected to remain within a favourable range or whether closer monitoring and potential irrigation planning may become necessary in the coming days.

5 Discussions

5.1 Benefits and limitations of data assimilation for operational forecasting

This pipeline demonstrates that integrating real-time observations, land surface modelling, data assimilation, and ensemble weather forecasts into a fully automated workflow can provide field-scale soil moisture forecasts with operational relevance. Data assimilation is expected to improve the representation of the system state at the forecast initialisation time; it can provide more accurate initial conditions and, consequently, improve subsequent forecast performance. Based on Figure 9, forecast agreement with CRNS observations is comparable or slightly better within the 2–5 day lead-time range than at shorter or longer lead times, while ensemble spread increases markedly beyond day 5, consistent with growing uncertainty in the atmospheric forcing. This behaviour is consistent with the established understanding that data assimilation primarily improves initial conditions, while forecast performance at longer lead times becomes increasingly constrained by the reliability of future atmospheric forcing (Crow and Ryu, 2009; Tian et al., 2021). This indicates that uncertainty in meteorological forcing remains the dominant limitation for operational soil moisture forecasting. Even when model states are well constrained through assimilation, errors in forecasted rainfall rapidly propagate into soil moisture predictions. Similar findings have been reported for hydrological prediction systems, where meteorological forcing is consistently identified as one of the largest sources of forecast uncertainty

https://doi.org/10.5194/egusphere-2026-4630
Preprint. Discussion started: 6 August 2026

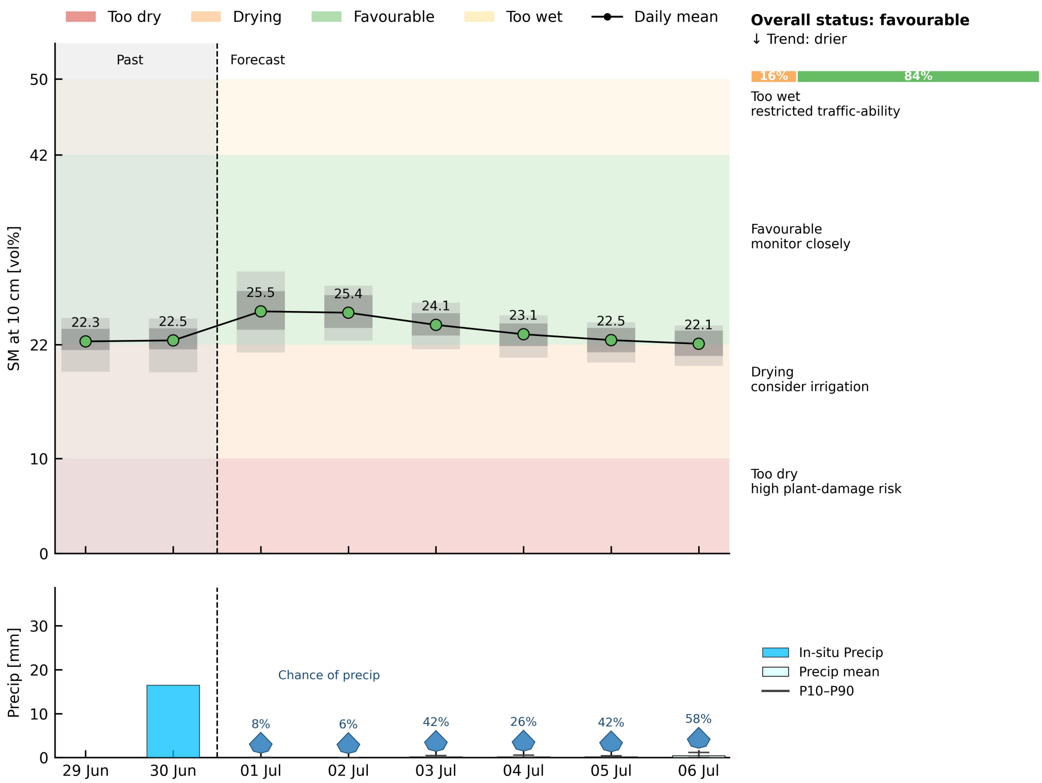

Figure 10. Intuitive visualization of probabilistic short-term 10 cm soil moisture (SM) forecast, translating ensemble-mean soil moisture into management-relevant categories (too dry, drying, good, too wet). Shaded boxes indicate the ensemble spread of the forecast$_{DA}$, with dark grey representing the interquartile range (P25–P75) and light grey the P10–P90 range. The lower panel shows ECMWF ENS mean precipitation, its P10–P90 range (error bars), and the daily precipitation probability (%).

(Dumedah and Walker, 2017; Gelati et al., 2018; Shrestha et al., 2020; Bai et al., 2024). Future improvements are therefore expected to arise from advances in precipitation forecasting, including higher-resolution convection-permitting ensemble forecasts (Cafaro et al., 2021), improved radar-NWP blending (Shehu and Haberlandt, 2022), and next-generation AI-assisted weather prediction systems (Lam et al., 2023). These developments have the potential to improve short-range rainfall forecasts and thereby extend the precision horizon of operational land surface forecasting.

Discrepancies between the soil moisture simulated by assimilating CRNS estimates and the independent distributed point-scale sensor network (SoilNet) were observed. The largest discrepancies were found at shallow depths of 5 to 10 cm. However, Brogi et al. (2025) showed for this site that the temporary removal and re-installation of point-scale sensors during field operations, especially in potato, can alter measurement conditions due to a) soil disturbance and changes in bulk density, and b) the difficulty of characterizing the complex soil moisture distribution of potato ridges by using point-scale devices (Brogi et al., 2026). In this work, the use of CRNS-based estimates provides a clear advantage over point-scale in situ sensors because

https://doi.org/10.5194/egusphere-2026-4630
Preprint. Discussion started: 6 August 2026

they integrate soil-moisture information over a larger footprint, thereby better representing field-scale conditions. In addition, CRNS measurements are less strongly influenced by small-scale surface heterogeneity, such as soil roughness (Brogi et al., 2026; Desilets et al., 2010; Zreda et al., 2012). Smaller discrepancies were found at 50 and 100 cm depths, and future studies could investigate the combined use of CRNS and 1 m deep point-scale sensors that can be positioned in ways that do not require periodical re-installation. While it cannot be excluded that CRNS-based estimates were affected by the absence of a vegetation correction (Jakobi et al., 2018), the biomass influence of low-height crops is relatively small (McJannet et al., 2014) and cannot account for the above-mentioned discrepancies with point-scale sensors. Finally, recent studies showed that the Desilets et al. (2010) method for CRNS-based soil moisture estimation is outperformed by the more recent Universal Transfer Solution (UTS) of Köhli et al. (2021) in low soil moisture conditions (i.e., below 10%). While soil moisture in this study was generally higher (i.e., above 15%), future applications in irrigation should favour the implementation of the UTS approach, for example, with user-friendly tools like Neptoon (Power et al., 2025).

The translation of probabilistic soil moisture forecasts into threshold-based indicators represents an important step toward operational usability. While ensemble forecasts provide a quantitative description of uncertainty, they are often difficult for non-expert users to interpret directly. Converting forecast outputs into management-relevant categories allows complex model information to be communicated in a simpler and more actionable form. In the presented case study, the thresholds are derived from site-specific knowledge of the Selhausen soil and from agriculturally relevant physical limits. The probabilistic presentation retains more information than a classification based only on the ensemble mean. In addition to the overall field status, the fraction of ensemble members assigned to each category indicates the probability of alternative field conditions. This is particularly important when forecasts lie close to a threshold. For example, an ensemble mean may remain within the favourable range while a non-negligible proportion of members already enters the drying category. Reporting these probabilities avoids the false impression of a deterministic classification and provides a clearer indication of forecast risk. Nevertheless, threshold-based indicators may conceal differences in the shape and spread of the underlying ensemble distribution, and small changes near a boundary may shift individual members into a different class even when their absolute differences are minor. Appropriate thresholds may vary with soil properties, crop type, rooting characteristics, and local management objectives. For a given crop, water requirements may also change during the growing season as a function of phenological development. In operational applications, threshold selection could be refined further by accounting for crop value, irrigation costs, water availability, and users' risk preferences. Such extensions would require closer integration with crop, economic, and behavioural decision models and are beyond the scope of the present study. Nevertheless, this pipeline aligns with recent developments in climate services and agricultural decision-support systems, which increasingly emphasize the importance of tailoring scientific information to user needs rather than providing raw model outputs alone. Translating model outputs into simplified, threshold-based indicators improves interpretability and highlights the potential to bridge the gap between scientific modelling and practical decision-making.

https://doi.org/10.5194/egusphere-2026-4630
Preprint. Discussion started: 6 August 2026

5.2 Transferability of the proposed pipeline

Although the pipeline is demonstrated at a single agricultural site in Germany, its overall architecture is designed to be transferable as these modular components are widely available, including observation acquisition, quality control, LSMs, sequential data assimilation, ensemble numerical weather prediction, probabilistic forecasting, and decision-oriented post-processing. The implementation is not restricted to an automated in situ monitoring system. Where continuous field observations are unavailable, state variables can be constrained using Earth observation products together with operational meteorological forcing datasets. For example, Sentinel-1 synthetic aperture radar (SAR) observations, which provide high spatial resolution soil moisture information estimates at revisit intervals of several days, have been widely used to retrieve surface soil moisture for assimilation into LSMs (Lievens et al., 2017; Bechtold et al., 2023). Likewise, meteorological forcing can be obtained from operational reanalysis or numerical weather prediction products, such as ERA5-Land. Therefore, the proposed pipeline can be modified and applied in data-sparse agricultural regions.

More importantly, the pipeline is not limited to soil moisture forecasting. The assimilation-forecasting workflow is generic and can be extended to other land surface variables for which observations and model representations exist. Recent land data assimilation systems increasingly perform multivariate assimilation (Lannoy et al., 2022), by jointly assimilating variables such as evapotranspiration (Gavahi et al., 2020), vegetation water content (Heyvaert et al., 2024), snow cover or snow water equivalent (Brangers et al., 2024; Lee et al., 2024), leaf area index (Wang et al., 2024; Heyvaert et al., 2024; Chakraborty and Saharia, 2025) and land surface temperature (Dumedah et al., 2011; Lu et al., 2020) to improve the simulated terrestrial water, energy, and carbon cycles. Such extensions would enable integration forecasting of water availability, crop development, and surface fluxes exchanges, thereby supporting a broader range of agricultural and environmental decision-making applications.

While the pipeline is broadly transferable, the forecast skill achieved in this study should not be interpreted as universally applicable. The predictive skill of such systems depends on the characteristics of the local environmental system and the quality of both observations and atmospheric forcing. Regions characterized by highly convective precipitation and complex topography are likely to exhibit larger forecast uncertainty (Matsunobu et al., 2024). Also, environmental characteristics influence forecast skill through their control on soil moisture memory. Fine-textured soils with high water-holding capacity generally have longer memory than coarse-textured soils with rapid drainage (Rahmati et al., 2024), allowing information introduced through data assimilation to persist over longer periods. Vegetation and land management further modulate soil moisture dynamics through their influence on evapotranspiration and root water uptake. Overall, the transferability of forecast skill is expected to depend on regional climate, soil characteristics, land cover, and agricultural management. Site-specific calibration of both the land surface model and the observation operator, therefore remains necessary to account for local soil hydraulic properties, vegetation characteristics, and management practices while reducing systematic model biases.

5.3 Future developments

Despite the advances shown in this study, the framework still represents agricultural management in a simplified manner. While ongoing developments in CLM are improving the representation of agricultural processes such as irrigation, fertilization, and

https://doi.org/10.5194/egusphere-2026-4630
Preprint. Discussion started: 6 August 2026

crop-specific dynamics, management operations are still largely prescribed rather than dynamically adjusted. For example, recent work on irrigation schemes demonstrates progress toward more realistic process-based representations within CLM (Dombrowski et al., 2024), yet these approaches do not explicitly account for adaptive farmer behavior. In practice, agricultural management is dynamic and evolves in response to weather conditions, forecast information, economic constraints, and individual risk preferences (Chavas and Shi, 2015). Farmers continuously adjust decisions such as irrigation timing or field operations based on both short-term conditions and long-term expectations, as well as insights from years of hands-on farming experience. Short-term irrigation decisions may be limited by factors such as the rotation of mobile pumps among several fields or shared access to wells, whereas longer-term decisions depend on water availability, expected crop value, and seasonal production objectives. Moreover, the present classification scheme applies fixed soil moisture thresholds, although crop water requirements vary with crop type and phenological stage. Future forecasting systems could therefore incorporate crop- and development-stage-specific thresholds together with locally relevant operational and resource constraints.

Recent developments in socio-hydrological and agent-based modelling increasingly address such feedbacks by coupling human decision-making processes with environmental models, enabling evaluation not only of how environmental conditions evolve, but also of how management decisions both influence and respond to those conditions. Building on this, the probabilistic soil moisture forecasts generated by the current framework could serve as inputs to such behavioural or agent-based decision models, allowing the current framework to be extended toward simulating adaptive management strategies and evaluating the full decision loop (Bruijn et al., 2023). This would enable assessment of not only forecast skill, but also the practical value of forecasts, i.e., how forecast information shapes management actions and subsequent soil moisture dynamics, in supporting adaptive land and water management under uncertainty.

6 Conclusion

This study presents an automated, end-to-end pipeline for operational, site-specific soil moisture forecasting that integrates real-time sensor observations, cloud-based data processing, the Community Land Model 5 (CLM5) land surface model, data assimilation via Ensemble Kalman Filter (EnKF), and ensemble weather forecasts to generate probabilistic 10-day predictions of soil moisture and related hydrological variables. By coupling near real-time observations with physically based modelling, the system enables continuous updating of model states and improved short-term predictive skill. Application at the Selhausen site showed that assimilating Cosmic-Ray Neutron Sensing (CRNS) observations reduced the discrepancy between modelled and observed soil moisture compared with the open-loop (OL) simulation, thereby providing more reliable initial conditions for forecasting. For the example forecast analysed here, ensemble spread relative to CRNS observations was comparable between the OL and Data assimilation (DA) initialized forecasts at short lead times, converged to their lowest values around lead days 2–4, and diverged again at longer lead times ($\geq$ 6 days), with ensemble spread increasing as uncertainty in the atmospheric forcing accumulated. The study further demonstrated that translating probabilistic forecasts into threshold-based soil moisture categories can improve interpretability and facilitate the communication of forecast information for agricultural management. Overall, this pipeline indicates that operational field-scale soil moisture forecasting is technically feasible

https://doi.org/10.5194/egusphere-2026-4630
Preprint. Discussion started: 6 August 2026

using currently available sensing, modelling, and forecasting technologies, providing a practical foundation that bridges the gap between climate services and operational agricultural decision support. Extending the framework from individual fields to larger regions is a promising but non-trivial next step. Satellite observations represent near-surface soil moisture and remain sensitive to vegetation, surface roughness, and retrieval assumptions, and their temporal sampling is also lower than that of in situ sensors. Future work should therefore evaluate multi-scale and multi-variable implementations that combine satellite observations with sparse in situ monitoring, high-resolution meteorological forcing, and land surface models. Priorities include reducing forcing uncertainties, quantifying uncertainty introduced by remotely sensed observations, improving representation of soil–vegetation–management interactions, and incorporating adaptive decision-making to capture more fully the socio-hydrological feedbacks inherent in agricultural systems. As climate variability and water-related risks continue to intensify, such integrated forecasting systems could become a key component of climate-resilient and climate-smart agricultural management and adaptation strategies.

Code availability. The model code and associated release are archived on Zenodo at https://doi.org/10.5281/zenodo.21487233. The scripts used to perform the experiments, process and analyse the data, and generate the figures presented in this study are available on Zenodo at https://doi.org/10.5281/zenodo.21720800 (Zhao et al., 2026b)

Data availability. Soil water content measurements for the Selhausen site are openly available through the TERENO Data Portal (https://ddp.tereno.net/ddp/) and can be accessed via https://hdl.handle.net/20.500.11952/TERENO/1056009548 (Bogena and Pütz, 2026).

Author contributions. HZ and RH contributed to the methodology, conducted the simulations, performed the data analysis and visualization, and contributed to the manuscript. HB and HJHF contributed to the methodology, conceptualization, manuscript, and supervision; HJHF also acquired funding. CB, AB, and KG contributed to the manuscript, and CB also contributed to visualization. JK and LS contributed software.

Competing interests. The authors declare that they have no known competing interests.

Acknowledgements. The research was conducted within the framework of the WATERAGRI project, which is funded by the European Union's Horizon 2020 research and innovation programme under grant agreement No 858375. The authors gratefully acknowledge the continuous exchange with stakeholders involved in the WATERAGRI project, as well as the valuable feedback, interest, and support from external stakeholders. We also thank the ICOS ETC team at Forschungszentrum Jülich (Alexander Graf, Nils Becker, and Andreas Haustein) for their work in operating the Selhausen station and for providing detailed and refined data products, which significantly contributed to our research. We further acknowledge the computing time provided on the JUWELS supercomputer at the Juelich Supercomputing Centre (JSC)

https://doi.org/10.5194/egusphere-2026-4630
Preprint. Discussion started: 6 August 2026

and the support of the TERENO (TERrestrial EnviroNmental Observatories) infrastructure funded by the Helmholtz Association. Harrie-Jan Hendricks-Franssen acknowledges funding from ESA (project SaveCrops4EU).

https://doi.org/10.5194/egusphere-2026-4630
Preprint. Discussion started: 6 August 2026

References

Aaheim, A., Amundsen, H., Dokken, T., and Wei, T.: Impacts and adaptation to climate change in European economies, Global Environmental Change, 22, 959–968, https://doi.org/10.1016/J.GLOENVCHA.2012.06.005, 2012.

Alavi, N., Warland, J. S., and Berg, A. A.: Assimilation of Soil Moisture and Temperature Data into Land Surface Models: A Survey, Data Assimilation for Atmospheric, Oceanic and Hydrologic Applications, pp. 429–448, https://doi.org/10.1007/978-3-540-71056-1_22, 2009.

Alwis, S. D., Hou, Z., Zhang, Y., Na, M. H., Ofoghi, B., and Sajjanhar, A.: A survey on smart farming data, applications and techniques, Computers in Industry, 138, 103 624, https://doi.org/10.1016/J.COMPIND.2022.103624, 2022.

Andreasen, M., Jensen, K. H., Desilets, D., Franz, T. E., Zreda, M., Bogena, H. R., and Looms, M. C.: Status and Perspectives on the Cosmic-Ray Neutron Method for Soil Moisture Estimation and Other Environmental Science Applications, Vadose Zone Journal, 16, 1–11, https://doi.org/10.2136/VZJ2017.04.0086, 2017.

Baatz, R., Bogena, H. R., Franssen, H. J. H., Huisman, J. A., Montzka, C., and Vereecken, H.: An empirical vegetation correction for soil water content quantification using cosmic ray probes, Water Resources Research, 51, 2030–2046, https://doi.org/10.1002/2014WR016443, 2015.

Bai, F., Wei, Z., Wei, N., Lu, X., Yuan, H., Zhang, S., Liu, S., Zhang, Y., Li, X., and Dai, Y.: Global Assessment of Atmospheric Forcing Uncertainties in The Common Land Model 2024 Simulations, Journal of Geophysical Research: Atmospheres, 129, e2024JD041 520, https://doi.org/10.1029/2024JD041520, 2024.

Bechtold, M., Modanesi, S., Lievens, H., Baguis, P., Brangers, I., Carrassi, A., Getirana, A., Gruber, A., Heyvaert, Z., Massari, C., Scherrer, S., Vannitsem, S., and Lannoy, G. D.: Assimilation of Sentinel-1 Backscatter into a Land Surface Model with River Routing and Its Impact on Streamflow Simulations in Two Belgian Catchments, Journal of Hydrometeorology, 24, 2389–2408, https://doi.org/10.1175/JHM-D-22-0198.1, 2023.

Belleflamme, A., Goergen, K., Wagner, N., Kollet, S., Bathiany, S., Zohbi, J. E., Rechid, D., Vanderborght, J., and Vereecken, H.: Hydrological forecasting at impact scale: the integrated ParFlow hydrological model at 0.6 km for climate resilient water resource management over Germany, Frontiers in Water, 5, 1183 642, https://doi.org/10.3389/FRWA.2023.1183642/TEXT, 2023.

Boas, T., Bogena, H., Grünwald, T., Heinesch, B., Ryu, D., Schmidt, M., Vereecken, H., Western, A., and Franssen, H. J. H.: Improving the representation of cropland sites in the Community Land Model (CLM) version 5.0, Geoscientific Model Development, 14, 573–601, https://doi.org/10.5194/GMD-14-573-2021, 2021.

Bogena, H. and Pütz, T.: Selhausen Germany Cosmic-Ray Neutron Probe (SE_C_001), TERENO Data Discovery Portal, Forschungszentrum Jülich, https://hdl.handle.net/20.500.11952/TERENO/1056009548, last access: 31 July 2026, 2026.

Bogena, H. R., Huisman, J. A., Schilling, B., Weuthen, A., and Vereecken, H.: Effective Calibration of Low-Cost Soil Water Content Sensors, Sensors 2017, Vol. 17,, 17, https://doi.org/10.3390/S17010208, 2017.

Bogena, H. R., Montzka, C., Huisman, J. A., Graf, A., Schmidt, M., Stockinger, M., Hebel, C. V., Hendricks-Franssen, H. J., Kruk, J. V. D., Tappe, W., Lücke, A., Baatz, R., Bol, R., Groh, J., Pütz, T., Jakobi, J., Kunkel, R., Sorg, J., Vereecken, H., Bogena, C. ., and Huis-Man, J. A.: The TERENO-Rur Hydrological Observatory: A Multiscale Multi-Compartment Research Platform for the Advancement of Hydrological Science, Vadose Zone Journal, 17, 1–22, https://doi.org/10.2136/VZJ2018.03.0055, 2018.

Bogena, H. R., Schrön, M., Jakobi, J., Ney, P., Zacharias, S., Andreasen, M., Baatz, R., Boorman, D., Duygu, M. B., Eguibar-Galán, M. A., Fersch, B., Franke, T., Geris, J., Sanchis, M. G., Kerr, Y., Korf, T., Mengistu, Z., Mialon, A., Nasta, P., Nitychoruk, J., Pisinaras, V., Rasche, D., Rosolem, R., Said, H., Schattan, P., Zreda, M., Achleitner, S., Albentosa-Hernández, E., Akyürek, Z., Blume, T., Campo,

https://doi.org/10.5194/egusphere-2026-4630
Preprint. Discussion started: 6 August 2026

A. D., Canone, D., Dimitrova-Petrova, K., Evans, J. G., Ferraris, S., Frances, F., Gisolo, D., Güntner, A., Herrmann, F., Iwema, J., Jensen, K. H., Kunstmann, H., Lidón, A., Looms, M. C., Oswald, S., Panagopoulos, A., Patil, A., Power, D., Rebmann, C., Romano, N., Scheiffele, L., Seneviratne, S., Weltin, G., and Vereecken, H.: COSMOS-Europe: a European network of cosmic-ray neutron soil moisture sensors, Earth System Science Data, 14, 1125–1151, https://doi.org/10.5194/ESSD-14-1125-2022, 2022a.

Bogena, H. R., Weuthen, A., and Huisman, J. A.: Recent Developments in Wireless Soil Moisture Sensing to Support Scientific Research and Agricultural Management, Sensors 2022, Vol. 22,, 22, https://doi.org/10.3390/S22249792, 2022b.

Bojovic, D., Clair, A. L. S., Christel, I., Terrado, M., Stanzel, P., Gonzalez, P., and Palin, E. J.: Engagement, involvement and empowerment: Three realms of a coproduction framework for climate services, Global Environmental Change, 68, 102 271, https://doi.org/10.1016/J.GLOENVCHA.2021.102271, 2021.

Brangers, I., Lievens, H., Getirana, A., and Lannoy, G. J. D.: Sentinel-1 Snow Depth Assimilation to Improve River Discharge Estimates in the Western European Alps, Water Resources Research, 60, e2023WR035 019, https://doi.org/10.1029/2023WR035019, 2024.

Brinkhoff, J., Hornbuckle, J., and Lurbe, C. B.: Soil moisture forecasting for irrigation recommendation, IFAC-PapersOnLine, 52, 385–390, https://doi.org/10.1016/J.IFACOL.2019.12.586, 2019.

Brogi, C., Huisman, J. A., Pätzold, S., von Hebel, C., Weihermüller, L., Kaufmann, M. S., van der Kruk, J., and Vereecken, H.: Large-scale soil mapping using multi-configuration EMI and supervised image classification, Geoderma, 335, 133–148, https://doi.org/10.1016/J.GEODERMA.2018.08.001, 2019.

Brogi, C., Huisman, J. A., Weihermüller, L., Herbst, M., and Vereecken, H.: Added value of geophysics-based soil mapping in agro-ecosystem simulations, SOIL, 7, 125–143, https://doi.org/10.5194/soil-7-125-2021, 2021.

Brogi, C., Bogena, H. R., Köhli, M., Huisman, J. A., Franssen, H. J. H., and Dombrowski, O.: Feasibility of irrigation monitoring with cosmic-ray neutron sensors, Geoscientific Instrumentation, Methods and Data Systems, 11, 451–469, https://doi.org/10.5194/GI-11-451-2022, 2022.

Brogi, C., Pisinaras, V., Köhli, M., Dombrowski, O., Franssen, H. J. H., Babakos, K., Chatzi, A., Panagopoulos, A., and Bogena, H. R.: Monitoring Irrigation in Small Orchards with Cosmic-Ray Neutron Sensors, Sensors, 23, https://doi.org/10.3390/S23052378/S1, 2023.

Brogi, C., Jakobi, J., Huisman, J. A., Schmidt, M., Montzka, C., Bates, J. S., Akter, S., and Bogena, H. R.: Cosmic-ray neutron sensors provide scale-appropriate soil water content and vegetation observations for eddy covariance stations in agricultural ecosystems, Agricultural and Forest Meteorology, 373, 110 731, https://doi.org/10.1016/J.AGRFORMET.2025.110731, 2025.

Brogi, C., Nieberding, F., Scheiffele, L., Daccache, A., Schrön, M., and Bogena, H. R.: Irrigation Monitoring With Cosmic-Ray Neutron Sensors: Unraveling Field Experiments With Neutron Transport Simulations, Water Resources Research, 62, e2025WR043 105, https://doi.org/10.1029/2025WR043105, 2026.

Bruijn, J. A. D., Smilovic, M., Burek, P., Guillaumot, L., Wada, Y., and Aerts, J. C.: GEB v0.1: a large-scale agent-based socio-hydrological model - simulating 10 million individual farming households in a fully distributed hydrological model, Geoscientific Model Development, 16, 2437–2454, https://doi.org/10.5194/GMD-16-2437-2023, 2023.

Bwambale, E., Naangmenyele, Z., Iradukunda, P., Agboka, K. M., Houessou-Dossou, E. A., Akansake, D. A., Bisa, M. E., Hamadou, A. A. H., Hakizayezu, J., Onofua, O. E., and Chikabvumbwa, S. R.: Towards precision irrigation management: A review of GIS, remote sensing and emerging technologies, Cogent Engineering, 9, https://doi.org/10.1080/23311916.2022.2100573, 2022.

Cafaro, C., Woodhams, B. J., Stein, T. H., Birch, C. E., Webster, S., Bain, C. L., Hartley, A., Clarke, S., Ferrett, S., and Hill, P.: Do Convection-Permitting Ensembles Lead to More Skillful Short-Range Probabilistic Rainfall Forecasts over Tropical East Africa?, Weather and Forecasting, 36, 697–716, https://doi.org/10.1175/WAF-D-20-0172.1, 2021.

https://doi.org/10.5194/egusphere-2026-4630
Preprint. Discussion started: 6 August 2026

Casado-Rodríguez, J., WIART, C. C. D., Grimaldi, S., Zsoter, E., Baugh, C., Bosshard, N., Mikuličková, M., Pechlivanidis, I., Prudhomme, C., and Salamon, P.: Optimizing Warnings for Hydrologic Ensemble Prediction Systems for Improved Decision-Making, Journal of Hydrometeorology, 26, 675–689, https://doi.org/10.1175/JHM-D-24-0054.1, 2025.

Chakraborty, A. and Saharia, M.: Joint assimilation of satellite soil moisture and vegetation conditions improves estimates of gross primary production and evapotranspiration over South Asia, Agricultural and Forest Meteorology, 373, 110 765, https://doi.org/10.1016/J.AGRFORMET.2025.110765, 2025.

Chavas, J.-P. and Shi, G.: An Economic Analysis of Risk, Management, and Agricultural Technology, Journal of Agricultural and Resource Economics, 40, 63–79, http://www.jstor.org/stable/44131277, 2015.

Clapp, R. B. and Hornberger, G. M.: Empirical equations for some soil hydraulic properties, Water Resources Research, 14, 601–604, https://doi.org/10.1029/WR014I004P00601, 1978.

Colossi, B. R. and Tucci, C. E. M.: Ensemble long-term soil moisture forecast using hydrological modeling, RBRH, 25, e28, https://doi.org/10.1590/2318-0331.252020190036, 2020.

Crow, W. T. and Ryu, D.: A new data assimilation approach for improving runoff prediction using remotely-sensed soil moisture retrievals, Hydrology and Earth System Sciences, 13, 1–16, https://doi.org/10.5194/HESS-13-1-2009, 2009.

Desilets, D. and Zreda, M.: Spatial and temporal distribution of secondary cosmic-ray nucleon intensities and applications to in situ cosmogenic dating, Earth and Planetary Science Letters, 206, 21–42, https://doi.org/10.1016/S0012-821X(02)01088-9, 2003.

Desilets, D., Zreda, M., and Ferré, T. P.: Nature's neutron probe: Land surface hydrology at an elusive scale with cosmic rays, Water Resources Research, 46, 11 505, https://doi.org/10.1029/2009WR008726, 2010.

Dombrowski, O., Brogi, C., Franssen, H. J. H., Zanotelli, D., and Bogena, H.: CLM5-FruitTree: A new sub-model for deciduous fruit trees in the Community Land Model (CLM5), Geoscientific Model Development, 15, 5167–5193, https://doi.org/10.5194/GMD-15-5167-2022, 2022.

Dombrowski, O., Brogi, C., Franssen, H. J. H., Pisinaras, V., Panagopoulos, A., Swenson, S., and Bogena, H.: Land Surface Modeling as a Tool to Explore Sustainable Irrigation Practices in Mediterranean Fruit Orchards, Water Resources Research, 60, e2023WR036 139, https://doi.org/10.1029/2023WR036139, 2024.

Dumedah, G. and Walker, J. P.: Assessment of model behavior and acceptable forcing data uncertainty in the context of land surface soil moisture estimation, Advances in Water Resources, 101, 23–36, https://doi.org/10.1016/J.ADVWATRES.2017.01.001, 2017.

Dumedah, G., Berg, A. A., and Wineberg, M.: An Integrated Framework for a Joint Assimilation of Brightness Temperature and Soil Moisture Using the Nondominated Sorting Genetic Algorithm II, Journal of Hydrometeorology, 12, 1596–1609, https://doi.org/10.1175/JHM-D-10-05029.1, 2011.

Franz, T. E., Wahbi, A., Zhang, J., Vreugdenhil, M., Heng, L., Dercon, G., Strauss, P., Brocca, L., and Wagner, W.: Practical Data Products From Cosmic-Ray Neutron Sensing for Hydrological Applications, Frontiers in Water, 2, 506 753, https://doi.org/10.3389/FRWA.2020.00009/TEXT, 2020.

Freebairn, D. M., Ghahramani, A., Robinson, J. B., and McClymont, D. J.: A tool for monitoring soil water using modelling, on-farm data, and mobile technology, Environmental Modelling & Software, 104, 55–63, https://doi.org/10.1016/J.ENVSOFT.2018.03.010, 2018.

Fu, Z., Ciais, P., Prentice, I. C., Gentine, P., Makowski, D., Bastos, A., Luo, X., Green, J. K., Stoy, P. C., Yang, H., and Hajima, T.: Atmospheric dryness reduces photosynthesis along a large range of soil water deficits, Nature Communications 2022 13:1, 13, 989–, https://doi.org/10.1038/s41467-022-28652-7, 2022.

Gavahi, K., Abbaszadeh, P., Moradkhani, H., Zhan, X., and Hain, C.: Multivariate Assimilation of Remotely Sensed Soil Moisture and Evapotranspiration for Drought Monitoring, Journal of Hydrometeorology, 21, 2293–2308, https://doi.org/10.1175/JHM-D-20-0057.1, 2020.

Gehne, M., Hamill, T. M., Bates, G. T., Pegion, P., and Kolczynski, W.: Land Surface Parameter and State Perturbations in the Global Ensemble Forecast System, Monthly Weather Review, 147, 1319–1340, https://doi.org/10.1175/MWR-D-18-0057.1, 2019.

Gelati, E., Decharme, B., Calvet, J. C., Minvielle, M., Polcher, J., Fairbairn, D., and Weedon, G. P.: Hydrological assessment of atmospheric forcing uncertainty in the Euro-Mediterranean area using a land surface model, Hydrology and Earth System Sciences, 22, 2091–2115, https://doi.org/10.5194/HESS-22-2091-2018, 2018.

Gevaert, A. I., Miralles, D. G., de Jeu, R. A., Schellekens, J., and Dolman, A. J.: Soil Moisture-Temperature Coupling in a Set of Land Surface Models, Journal of Geophysical Research: Atmospheres, 123, 1481–1498, https://doi.org/10.1002/2017JD027346, 2018.

Google and Maxar Technologies: Satellite imagery of Germany, Google Maps/Google Earth, https://maps.google.com, accessed: [your access date], 2020.

Google and Maxar Technologies: Satellite imagery of Germany, Google Maps/Google Earth, https://maps.google.com, accessed: [your access date], 2022.

Graf, A., Klosterhalfen, A., Arriga, N., Bernhofer, C., Bogena, H., Bornet, F., Brüggemann, N., Brümmer, C., Buchmann, N., Chi, J., Chipeaux, C., Cremonese, E., Cuntz, M., Dušek, J., El-Madany, T. S., Fares, S., Fischer, M., Foltýnová, L., Gharun, M., Ghiasi, S., Gielen, B., Gottschalk, P., Grünwald, T., Heinemann, G., Heinesch, B., Heliasz, M., Holst, J., Hörtnagl, L., Ibrom, A., Ingwersen, J., Jurasinski, G., Klatt, J., Knohl, A., Koebsch, F., Konopka, J., Korkiakoski, M., Kowalska, N., Kremer, P., Kruijt, B., Lafont, S., Léonard, J., Ligne, A. D., Longdoz, B., Loustau, D., Magliulo, V., Mammarella, I., Manca, G., Mauder, M., Migliavacca, M., Mölder, M., Neirynck, J., Ney, P., Nilsson, M., Paul-Limoges, E., Peichl, M., Pitacco, A., Poyda, A., Rebmann, C., Roland, M., Sachs, T., Schmidt, M., Schrader, F., Siebicke, L., Šigut, L., Tuittila, E. S., Varlagin, A., Vendrame, N., Vincke, C., Völksch, I., Weber, S., Wille, C., Wizemann, H. D., Zeeman, M., and Vereecken, H.: Altered energy partitioning across terrestrial ecosystems in the European drought year 2018: Energy partitioning in the drought 2018, Philosophical Transactions of the Royal Society B: Biological Sciences, 375, 14 473, https://doi.org/10.1098/RSTB.2019.0524/31297, 2020.

Gumiere, S. J., Camporese, M., Botto, A., Lafond, J. A., Paniconi, C., Gallichand, J., and Rousseau, A. N.: Machine Learning vs. Physics-Based Modeling for Real-Time Irrigation Management, Frontiers in Water, 2, 515 703, https://doi.org/10.3389/FRWA.2020.00008/TEXT, 2020.

Han, X., Franssen, H. J. H., Montzka, C., and Vereecken, H.: Soil moisture and soil properties estimation in the Community Land Model with synthetic brightness temperature observations, Water Resources Research, 50, 6081–6105, https://doi.org/10.1002/2013WR014586, 2014.

Hawdon, A., McJannet, D., and Wallace, J.: Calibration and correction procedures for cosmic-ray neutron soil moisture probes located across Australia, Water Resources Research, 50, 5029–5043, https://doi.org/10.1002/2013WR015138, 2014.

Hendrickx, M. G., Vanderborght, J., Janssens, P., Laloy, E., Bombeke, S., Matthyssen, E., Waverijn, A., and Diels, J.: Field-Scale Soil Moisture Predictions in Real Time Using In Situ Sensor Measurements in an Inverse Modeling Framework: SWIM2, Water Resources Research, 62, e2025WR041 324, https://doi.org/10.1029/2025WR041324, 2026.

Heyvaert, Z., Scherrer, S., Dorigo, W., Bechtold, M., and Lannoy, G. D.: Joint assimilation of satellite-based surface soil moisture and vegetation conditions into the Noah-MP land surface model, Science of Remote Sensing, 9, 100 129, https://doi.org/10.1016/J.SRS.2024.100129, 2024.

Jakobi, J., Huisman, J. A., Vereecken, H., Diekkrüger, B., and Bogena, H. R.: Cosmic Ray Neutron Sensing for Simultaneous Soil Water Content and Biomass Quantification in Drought Conditions, Water Resources Research, 54, 7383–7402, https://doi.org/10.1029/2018WR022692, 2018.

Jakobi, J., Huisman, J. A., Schrön, M., Fiedler, J., Brogi, C., Vereecken, H., and Bogena, H. R.: Error Estimation for Soil Moisture Measurements With Cosmic Ray Neutron Sensing and Implications for Rover Surveys, Frontiers in Water, 2, 529 308, https://doi.org/10.3389/FRWA.2020.00010/TEXT, 2020.

Jarvis, N., Groh, J., Lewan, E., Meurer, K. H., Durka, W., Baessler, C., Pütz, T., Rufullayev, E., and Vereecken, H.: Coupled modelling of hydrological processes and grassland production in two contrasting climates, Hydrology and Earth System Sciences, 26, 2277–2299, https://doi.org/10.5194/HESS-26-2277-2022, 2022.

Jin, N., Tao, B., Ren, W., He, L., Zhang, D., Wang, D., and Yu, Q.: Assimilating remote sensing data into a crop model improves winter wheat yield estimation based on regional irrigation data, Agricultural Water Management, 266, 107 583, https://doi.org/10.1016/J.AGWAT.2022.107583, 2022.

Karandish, F. and Šimůnek, J.: A comparison of numerical and machine-learning modeling of soil water content with limited input data, Journal of Hydrology, 543, 892–909, https://doi.org/10.1016/J.JHYDROL.2016.11.007, 2016.

Kay, J. E., Deser, C., Phillips, A., Mai, A., Hannay, C., Strand, G., Arblaster, J. M., Bates, S. C., Danabasoglu, G., Edwards, J., Holland, M., Kushner, P., Lamarque, J. F., Lawrence, D., Lindsay, K., Middleton, A., Munoz, E., Neale, R., Oleson, K., Polvani, L., and Vertenstein, M.: The Community Earth System Model (CESM) Large Ensemble Project: A Community Resource for Studying Climate Change in the Presence of Internal Climate Variability, Bulletin of the American Meteorological Society, 96, 1333–1349, https://doi.org/10.1175/BAMS-D-13-00255.1, 2015.

Klages, S., Heidecke, C., and Osterburg, B.: The Impact of Agricultural Production and Policy on Water Quality during the Dry Year 2018, a Case Study from Germany, Water 2020, Vol. 12,, 12, https://doi.org/10.3390/W12061519, 2020.

Korres, W., Reichenau, T. G., Fiener, P., Koyama, C. N., Bogena, H. R., Cornelissen, T., Baatz, R., Herbst, M., Diekkrüger, B., Vereecken, H., and Schneider, K.: Spatio-temporal soil moisture patterns – A meta-analysis using plot to catchment scale data, Journal of Hydrology, 520, 326–341, https://doi.org/10.1016/J.JHYDROL.2014.11.042, 2015.

Kurtz, W., He, G., Kollet, S. J., Maxwell, R. M., Vereecken, H., and Franssen, H. J. H.: TerrSysMP-PDAF (version 1.0): A modular high-performance data assimilation framework for an integrated land surface-subsurface model, Geoscientific Model Development, 9, 1341–1360, https://doi.org/10.5194/GMD-9-1341-2016, 2016.

Köhli, M.: Soil moisture measurements by Cosmic-Ray neutron sensing: A critical review, Geoderma, 465, 117 626, https://doi.org/10.1016/J.GEODERMA.2025.117626, 2026.

Köhli, M., Schrön, M., Zreda, M., Schmidt, U., Dietrich, P., and Zacharias, S.: Footprint characteristics revised for field-scale soil moisture monitoring with cosmic-ray neutrons, Water Resources Research, 51, 5772–5790, https://doi.org/10.1002/2015WR017169, 2015.

Köhli, M., Weimar, J., Schrön, M., Baatz, R., and Schmidt, U.: Soil Moisture and Air Humidity Dependence of the Above-Ground Cosmic-Ray Neutron Intensity, Frontiers in Water, 2, 544 847, https://doi.org/10.3389/FRWA.2020.544847/TEXT, 2021.

Lam, R., Sanchez-Gonzalez, A., Willson, M., Wirnsberger, P., Fortunato, M., Alet, F., Ravuri, S., Ewalds, T., Eaton-Rosen, Z., Hu, W., Merose, A., Hoyer, S., Holland, G., Vinyals, O., Stott, J., Pritzel, A., Mohamed, S., and Battaglia, P.: Learning skillful medium-range global weather forecasting, Science, 382, 1416–1422, https://doi.org/10.1126/SCIENCE.ADI2336/SUPPL_FILE/SCIENCE.ADI2336_SM.PDF, 2023.

Lannoy, G. J. D., Bechtold, M., Albergel, C., Brocca, L., Calvet, J. C., Carrassi, A., Crow, W. T., de Rosnay, P., Durand, M., Forman, B., Geppert, G., Girotto, M., Franssen, H. J. H., Jonas, T., Kumar, S., Lievens, H., Lu, Y., Massari, C., Pauwels, V. R., Reichle, R. H., and Steele-Dunne, S.: Perspective on satellite-based land data assimilation to estimate water cycle components in an era of advanced data availability and model sophistication, Frontiers in Water, 4, 981 745, https://doi.org/10.3389/FRWA.2022.981745/XML, 2022.

Lawrence, D. M., Fisher, R. A., Koven, C. D., Oleson, K. W., Swenson, S. C., Bonan, G., Collier, N., Ghimire, B., van Kampenhout, L., Kennedy, D., Kluzek, E., Lawrence, P. J., Li, F., Li, H., Lombardozzi, D., Riley, W. J., Sacks, W. J., Shi, M., Vertenstein, M., Wieder, W. R., Xu, C., Ali, A. A., Badger, A. M., Bisht, G., van den Broeke, M., Brunke, M. A., Burns, S. P., Buzan, J., Clark, M., Craig, A., Dahlin, K., Drewniak, B., Fisher, J. B., Flanner, M., Fox, A. M., Gentine, P., Hoffman, F., Keppel-Aleks, G., Knox, R., Kumar, S., Lenaerts, J., Leung, L. R., Lipscomb, W. H., Lu, Y., Pandey, A., Pelletier, J. D., Perket, J., Randerson, J. T., Ricciuto, D. M., Sanderson, B. M., Slater, A., Subin, Z. M., Tang, J., Thomas, R. Q., Martin, M. V., and Zeng, X.: The Community Land Model Version 5: Description of New Features, Benchmarking, and Impact of Forcing Uncertainty, Journal of Advances in Modeling Earth Systems, 11, 4245–4287, https://doi.org/10.1029/2018MS001583, 2019.

Lee, J., Lee, M. I., Tak, S., Seo, E., and Lee, Y. K.: Assimilation of snow water equivalent from AMSR2 and IMS satellite data utilizing the local ensemble transform Kalman filter, Geoscientific Model Development, 17, 8799–8816, https://doi.org/10.5194/GMD-17-8799-2024, 2024.

Li, D., Franssen, H. J. H., Han, X., Jiménez-Bello, M. A., Alzamora, F. M., and Vereecken, H.: Evaluation of an operational real-time irrigation scheduling scheme for drip irrigated citrus fields in Picassent, Spain, Agricultural Water Management, 208, 465–477, https://doi.org/10.1016/J.AGWAT.2018.06.022, 2018.

Li, F., Bogena, H. R., Bayat, B., Kurtz, W., and Franssen, H. J. H.: Can a Sparse Network of Cosmic Ray Neutron Sensors Improve Soil Moisture and Evapotranspiration Estimation at the Larger Catchment Scale?, Water Resources Research, 60, e2023WR035 056, https://doi.org/10.1029/2023WR035056, 2024.

Li, W., Awais, M., Ru, W., Shi, W., Ajmal, M., Uddin, S., and Liu, C.: Review of Sensor Network-Based Irrigation Systems Using IoT and Remote Sensing, Advances in Meteorology, 2020, 8396 164, https://doi.org/10.1155/2020/8396164, 2020.

Lievens, H., Reichle, R. H., Liu, Q., Lannoy, G. J. D., Dunbar, R. S., Kim, S. B., Das, N. N., Cosh, M., Walker, J. P., and Wagner, W.: Joint Sentinel-1 and SMAP data assimilation to improve soil moisture estimates, Geophysical Research Letters, 44, 6145–6153, https://doi.org/10.1002/2017GL073904, 2017.

Liu, X., Liu, W., Tang, Q., Liu, B., Wada, Y., and Yang, H.: Global Agricultural Water Scarcity Assessment Incorporating Blue and Green Water Availability Under Future Climate Change, Earth's Future, 10, e2021EF002 567, https://doi.org/10.1029/2021EF002567, 2022.

Lobell, D. B. and Gourdji, S. M.: The Influence of Climate Change on Global Crop Productivity, Plant Physiology, 160, 1686, https://doi.org/10.1104/PP.112.208298, 2012.

Lu, X., Groh, J., Graf, A., Pütz, T., Gerke, H. H., Gründling, R., Rupp, H., Kiese, R., Vogel, H. J., Javaux, M., Vereecken, H., and Franssen, H. J. H.: Robustness of critical soil moisture to curve-fitting methods and its variability with soil depth, soil texture, and climatic conditions: insights from lysimeter data in Germany, Journal of Hydrology, 668, 134 959, https://doi.org/10.1016/J.JHYDROL.2026.134959, 2026.

Lu, Y., Steele-Dunne, S. C., and Lannoy, G. J. D.: Improving Soil Moisture and Surface Turbulent Heat Flux Estimates by Assimilation of SMAP Brightness Temperatures or Soil Moisture Retrievals and GOES Land Surface Temperature Retrievals, Journal of Hydrometeorology, 21, 183–203, https://doi.org/10.1175/JHM-D-19-0130.1, 2020.

Ma, J., Li, R., Liu, H., Huang, Z., Wu, T., Wu, X., Zhao, L., Hu, G., Xiao, Y., Jiao, Y., Liu, W., Wang, S., Shi, J., and Qiao, Y.: Evaluation of CLM5.0 for simulating surface energy budget and soil hydrothermal regime in permafrost regions of the Qinghai-Tibet Plateau, Agricultural and Forest Meteorology, 332, 109 380, https://doi.org/10.1016/J.AGRFORMET.2023.109380, 2023.

Matsunobu, T., Puh, M., and Keil, C.: Flow- and scale-dependent spatial predictability of convective precipitation combining different model uncertainty representations, Quarterly Journal of the Royal Meteorological Society, 150, 2364–2381, https://doi.org/10.1002/QJ.4713, 2024.

McJannet, D., Franz, T., Hawdon, A., Boadle, D., Baker, B., Almeida, A., Silberstein, R., Lambert, T., and Desilets, D.: Field testing of the universal calibration function for determination of soil moisture with cosmic-ray neutrons, Water Resources Research, 50, 5235–5248, https://doi.org/10.1002/2014WR015513, 2014.

McMillan, H., Jackson, B., Clark, M., Kavetski, D., and Woods, R.: Rainfall uncertainty in hydrological modelling: An evaluation of multiplicative error models, Journal of Hydrology, 400, 83–94, https://doi.org/10.1016/J.JHYDROL.2011.01.026, 2011.

Nerger, L., Hiller, W., and Schröter, J.: PDAF - The parallel data assimilation framework: Experiences with kalman filtering, in: Proceedings of the 11th ECMWF Workshop on the Use of High Performance Computing in Meteorology, pp. 63–83, WORLD SCIENTIFIC, ISBN 9812563547, https://doi.org/10.1142/9789812701831_0006, 2005.

Ney, P., Kohli, M., Bogena, H., and Goergen, K.: CRNS-based monitoring technologies for a weather and climate-resilient agriculture: Realization by the ADAPTER project, 2021 IEEE International Workshop on Metrology for Agriculture and Forestry, MetroAgriFor 2021 - Proceedings, pp. 203–208, https://doi.org/10.1109/METROAGRIFOR52389.2021.9628766, 2021.

Nsoh, B., Katimbo, A., Guo, H., Heeren, D. M., Nakabuye, H. N., Qiao, X., Ge, Y., Rudnick, D. R., Wanyama, J., Bwambale, E., and Kiraga, S.: Internet of Things-Based Automated Solutions Utilizing Machine Learning for Smart and Real-Time Irrigation Management: A Review, Sensors 2024, Vol. 24,, 24, https://doi.org/10.3390/S24237480, 2024.

Ochsner, T. E., Cosh, M. H., Cuenca, R. H., Dorigo, W. A., Draper, C. S., Hagimoto, Y., Kerr, Y. H., Larson, K. M., Njoku, E. G., Small, E. E., and Zreda, M.: State of the Art in Large-Scale Soil Moisture Monitoring, Soil Science Society of America Journal, 77, 1888–1919, https://doi.org/10.2136/SSSAJ2013.03.0093, 2013.

Ollinaho, P., Carver, G. D., Lang, S. T., Tuppi, L., Ekblom, M., and Järvinen, H.: Ensemble prediction using a new dataset of ECMWF initial states-OpenEnsemble 1.0, Geoscientific Model Development, 14, 2143–2160, https://doi.org/10.5194/GMD-14-2143-2021, 2021.

Porter, J. J. and Dessai, S.: Mini-me: Why do climate scientists' misunderstand users and their needs?, Environmental Science & Policy, 77, 9–14, https://doi.org/10.1016/J.ENVSCI.2017.07.004, 2017.

Power, D., Zacharias, S., Erxleben, F., Rosolem, R., and Schrön, M.: neptoon: An extensible software tool for CRNS data processing, ARPHA Conference Abstracts 8: e158417, 8, e158 417, https://doi.org/10.3897/ACA.8.E158417, 2025.

Pulido-Bosch, A., Rigol-Sanchez, J. P., Vallejos, A., Andreu, J. M., Ceron, J. C., Molina-Sanchez, L., and Sola, F.: Impacts of agricultural irrigation on groundwater salinity, Environmental Earth Sciences, 77, 197–, https://doi.org/10.1007/S12665-018-7386-6/FIGURES/7, 2018.

Pütz, T., Kiese, R., Wollschläger, U., Groh, J., Rupp, H., Zacharias, S., Priesack, E., Gerke, H. H., Gasche, R., Bens, O., Borg, E., Baessler, C., Kaiser, K., Herbrich, M., Munch, J. C., Sommer, M., Vogel, H. J., Vanderborght, J., and Vereecken, H.: TERENO-SOILCan: a lysimeter-network in Germany observing soil processes and plant diversity influenced by climate change, Environmental Earth Sciences, 75, 1242–, https://doi.org/10.1007/S12665-016-6031-5/FIGURES/11, 2016.

Ragab, R., Evans, J. G., Battilani, A., and Solimando, D.: The Cosmic-ray Soil Moisture Observation System (Cosmos) for Estimating the Crop Water Requirement: New Approach†, Irrigation and Drainage, 66, 456–468, https://doi.org/10.1002/IRD.2152, 2017.

Rahmati, M., Amelung, W., Brogi, C., Dari, J., Flammini, A., Bogena, H., Brocca, L., Chen, H., Groh, J., Koster, R. D., McColl, K. A., Montzka, C., Moradi, S., Rahi, A., S., F. S., and Vereecken, H.: Soil Moisture Memory: State-Of-The-Art and the Way Forward, Reviews of Geophysics, 62, e2023RG000 828, https://doi.org/10.1029/2023RG000828, 2024.

Raza, A., Razzaq, A., Mehmood, S. S., Zou, X., Zhang, X., Lv, Y., and Xu, J.: Impact of Climate Change on Crops Adaptation and Strategies to Tackle Its Outcome: A Review, Plants 2019, Vol. 8,, 8, https://doi.org/10.3390/PLANTS8020034, 2019.

Reichle, R. H.: Data assimilation methods in the Earth sciences, Advances in Water Resources, 31, 1411–1418, https://doi.org/10.1016/J.ADVWATRES.2008.01.001, 2008.

Reichle, R. H., Koster, R. D., Liu, P., Mahanama, S. P., Njoku, E. G., and Owe, M.: Comparison and assimilation of global soil moisture retrievals from the Advanced Microwave Scanning Radiometer for the Earth Observing System (AMSR-E) and the Scanning Multichannel Microwave Radiometer (SMMR), Journal of Geophysical Research: Atmospheres, 112, 9108, https://doi.org/10.1029/2006JD008033, 2007.

Reichle, R. H., Kumar, S. V., Mahanama, S. P., Koster, R. D., and Liu, Q.: Assimilation of Satellite-Derived Skin Temperature Observations into Land Surface Models, Journal of Hydrometeorology, 11, 1103–1122, https://doi.org/10.1175/2010JHM1262.1, 2010.

Reichstein, M., Bahn, M., Ciais, P., Frank, D., Mahecha, M. D., Seneviratne, S. I., Zscheischler, J., Beer, C., Buchmann, N., Frank, D. C., Papale, D., Rammig, A., Smith, P., Thonicke, K., Velde, M. V. D., Vicca, S., Walz, A., and Wattenbach, M.: Climate extremes and the carbon cycle, Nature 2013 500:7462, 500, 287–295, https://doi.org/10.1038/nature12350, 2013.

Rosolem, R., Shuttleworth, W. J., Zreda, M., Franz, T. E., Zeng, X., and Kurc, S. A.: The Effect of Atmospheric Water Vapor on Neutron Count in the Cosmic-Ray Soil Moisture Observing System, Journal of Hydrometeorology, 14, 1659–1671, https://doi.org/10.1175/JHM-D-12-0120.1, 2013.

Rudolph, S., van der Kruk, J., von Hebel, C., Ali, M., Herbst, M., Montzka, C., Pätzold, S., Robinson, D. A., Vereecken, H., and Weihermüller, L.: Linking satellite derived LAI patterns with subsoil heterogeneity using large-scale ground-based electromagnetic induction measurements, Geoderma, 241-242, 262–271, https://doi.org/10.1016/J.GEODERMA.2014.11.015, 2015.

Sadri, S., Famiglietti, J. S., Pan, M., Beck, H. E., Berg, A., and Wood, E. F.: FarmCan: a physical, statistical, and machine learning model to forecast crop water deficit for farms, Hydrology and Earth System Sciences, 26, 5373–5390, https://doi.org/10.5194/HESS-26-5373-2022, 2022.

Schrön, M., Köhli, M., Scheiffele, L., Iwema, J., Bogena, H. R., Lv, L., Martini, E., Baroni, G., Rosolem, R., Weimar, J., Mai, J., Cuntz, M., Rebmann, C., Oswald, S. E., Dietrich, P., Schmidt, U., and Zacharias, S.: Improving calibration and validation of cosmic-ray neutron sensors in the light of spatial sensitivity, Hydrology and Earth System Sciences, 21, 5009–5030, https://doi.org/10.5194/HESS-21-5009-2017, 2017.

Shehu, B. and Haberlandt, U.: Improving radar-based rainfall nowcasting by a nearest-neighbour approach-Part 1: Storm characteristics, Hydrol. Earth Syst. Sci, 26, 1631–1658, https://doi.org/10.5194/hess-26-1631-2022, 2022.

Shrestha, A., Nair, A. S., and Indu, J.: Role of precipitation forcing on the uncertainty of land surface model simulated soil moisture estimates, Journal of Hydrology, 580, 124 264, https://doi.org/10.1016/J.JHYDROL.2019.124264, 2020.

Shrestha, P., Sulis, M., Masbou, M., Kollet, S., and Simmer, C.: A Scale-Consistent Terrestrial Systems Modeling Platform Based on COSMO, CLM, and ParFlow, Monthly Weather Review, 142, 3466–3483, https://doi.org/10.1175/MWR-D-14-00029.1, 2014.

Smith, A. P., Yung, L., Snitker, A. J., Bocinsky, R. K., Metcalf, E. C., and Jencso, K.: Scalar Mismatches and Underlying Factors for Underutilization of Climate Information: Perspectives From Farmers and Ranchers, Frontiers in Climate, 3, 663 071, https://doi.org/10.3389/FCLIM.2021.663071/BIBTEX, 2021.

https://doi.org/10.5194/egusphere-2026-4630
Preprint. Discussion started: 6 August 2026

Srivastav, A. L., Dhyani, R., Ranjan, M., Madhav, S., and Sillanpää, M.: Climate-resilient strategies for sustainable management of water resources and agriculture, Environmental Science and Pollution Research 2021 28:31, 28, 41 576–41 595, https://doi.org/10.1007/S11356-021-14332-4, 2021.

Strebel, L., Bogena, H. R., Vereecken, H., and Franssen, H. J. H.: Coupling the Community Land Model version 5.0 to the parallel data assimilation framework PDAF: Description and applications, Geoscientific Model Development, 15, 395–411, https://doi.org/10.5194/GMD-15-395-2022, 2022.

Tian, S., Renzullo, L. J., Pipunic, R. C., Lerat, J., Sharples, W., and Donnelly, C.: Satellite soil moisture data assimilation for improved operational continental water balance prediction, Hydrol. Earth Syst. Sci, 25, 4567–4584, https://doi.org/10.5194/hess-25-4567-2021, 2021.

Togneri, R., dos Santos, D. F., Camponogara, G., Nagano, H., Custódio, G., Prati, R., Fernandes, S., and Kamienski, C.: Soil moisture forecast for smart irrigation: The primetime for machine learning, Expert Systems with Applications, 207, 117 653, https://doi.org/10.1016/J.ESWA.2022.117653, 2022.

Topp, G. C., Davis, J. L., and Annan, A. P.: Electromagnetic determination of soil water content: Measurements in coaxial transmission lines, Water Resources Research, 16, 574–582, https://doi.org/10.1029/WR016I003P00574, 1980.

Turner, M. R., Walker, J. P., and Oke, P. R.: Ensemble member generation for sequential data assimilation, Remote Sensing of Environment, 112, 1421–1433, https://doi.org/10.1016/J.RSE.2007.02.042, 2008.

Veerachamy, R. and Ramar, R.: Agricultural Irrigation Recommendation and Alert (AIRA) system using optimization and machine learning in Hadoop for sustainable agriculture, Environmental Science and Pollution Research, 29, 19 955–19 974, https://doi.org/10.1007/S11356-021-13248-3/TABLES/8, 2022.

Viovy, N.: CRUNCEP Version 7 - Atmospheric Forcing Data for the Community Land Model, https://doi.org/10.5065/PZ8F-F017, 2018.

Wang, J., Bogena, H. R., Vereecken, H., and Brüggemann, N.: Stable-Isotope-Aided Investigation of the Effect of Redox Potential on Nitrous Oxide Emissions as Affected by Water Status and N Fertilization, Water 2020, Vol. 12,, 12, 1–20, https://doi.org/10.3390/W12102918, 2020.

Wang, W., Rong, Y., Zhang, C., Wang, C., and Huo, Z.: Data assimilation of soil moisture and leaf area index effectively improves the simulation accuracy of water and carbon fluxes in coupled farmland hydrological model, Agricultural Water Management, 291, 108 646, https://doi.org/10.1016/J.AGWAT.2023.108646, 2024.

Wieder, W. R., Knowles, J. F., Blanken, P. D., Swenson, S. C., and Suding, K. N.: Ecosystem function in complex mountain terrain: Combining models and long-term observations to advance process-based understanding, Journal of Geophysical Research: Biogeosciences, 122, 825–845, https://doi.org/10.1002/2016JG003704, 2017.

Yan, H., Sun, N., Eldardiry, H., Thurber, T. B., Reed, P. M., Malek, K., Gupta, R., Kennedy, D., Swenson, S. C., Hou, Z., Cheng, Y., and Rice, J. S.: Large Ensemble Diagnostic Evaluation of Hydrologic Parameter Uncertainty in the Community Land Model Version 5 (CLM5), Journal of Advances in Modeling Earth Systems, 15, e2022MS003 312, https://doi.org/10.1029/2022MS003312, 2023.

Zhao, H., Bhosale, R., and Wainwright, H. M.: A physics-guided sensor-to-model framework for real-time estimation and near-future forecasting of soil moisture, Advances in Water Resources, 209, 105 221, https://doi.org/10.1016/J.ADVWATRES.2026.105221, 2026a.

Zhao, H., Hoffmann, R., Bogena, H., Brogi, C., Belleflamme, A., Görgen, K., Keller, J., Strebel, L., and Hendricks Franssen, H.-J.: From Sensors to Irrigation Decisions: An Automated Data–Model Pipeline for Real-Time Soil Moisture Forecasting in Agriculture, https://doi.org/10.5281/zenodo.21720800, 2026b.

https://doi.org/10.5194/egusphere-2026-4630
Preprint. Discussion started: 6 August 2026

Zreda, M., Desilets, D., Ferré, T. P., and Scott, R. L.: Measuring soil moisture content non-invasively at intermediate spatial scale using cosmic-ray neutrons, Geophysical Research Letters, 35, https://doi.org/10.1029/2008GL035655, 2008.

Zreda, M., Shuttleworth, W. J., Zeng, X., Zweck, C., Desilets, D., Franz, T., and Rosolem, R.: COSMOS: The cosmic-ray soil moisture observing system, Hydrology and Earth System Sciences, 16, 4079–4099, https://doi.org/10.5194/HESS-16-4079-2012, 2012.